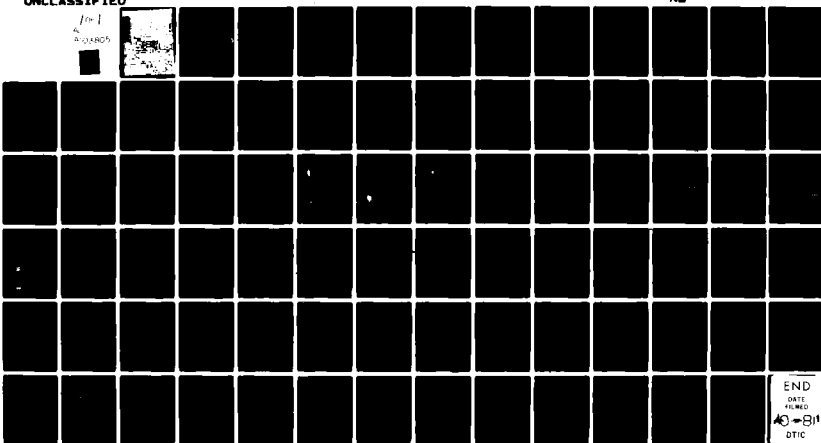


AD-A103 805 MICHIGAN STATE UNIV EAST LANSING DIV OF ENGINEERING --ETC F/6 17/9
RADAR WAVEFORM SYNTHESIS FOR TARGET IDENTIFICATION (U)
JUN 81 K CHEN N00019-80-K-0362
NL

UNCLASSIFIED

100-1
4-03626



END
DATE FILMED
40-81
DTIC

AD A103805

17411-1

12

Final Report, 5 May 80 - 4 May 81

61 RADAR WAVEFORM SYNTHESIS FOR TARGET IDENTIFICATION

12-1
Naval Air System Command
Contract No. N00019-80-K-0382

11-1 June 1
Reporting period
May 5, 1980 to May 4, 1981

DTIC
S 21 SEP 2 1981 D
H

Prepared by

16 Kun-Mu Chen Principal Investigator

Division of Engineering Research
College of Engineering
Michigan State University
East Lansing, Michigan 48824

APPROVED FOR PUBLIC RELEASE
DISTRIBUTION UNLIMITED

431 0-6

RADAR WAVEFORM SYNTHESIS FOR TARGET IDENTIFICATION

Abstract

A new scheme for radar detection and discrimination, the radar waveform synthesis method, is investigated. This scheme consists of synthesizing an aspect-independent waveform for the incident radar signal which excites an arbitrarily oriented target in such a way that the return radar signal from the target contains only a single natural resonance mode of the target in the late-time period. When the synthesized incident radar signal for exciting a particular natural mode of a known, preselected target is applied to a wrong target, the return radar signal will be significantly different from that of the expected natural mode, thus, the wrong target can be sensitively discriminated. The selection of an optimum pulse duration of the required incident signal for the purpose of shaping its waveform is also studied.

Three kinds of targets, an arbitrarily oriented thin wire, a sphere and a normally oriented infinite cylinder, have been investigated. The cases of an arbitrarily oriented wire and a sphere have been completed and the results are reported in Parts 1 and 2. The case of infinite cylinder will be completed shortly and incomplete results of this case are outlined in Part 3.

Accession For	NTIS GRAIL
DTIC	13
UNCLASSIFIED	
Journal	100
Pub	100
Distribution	100
Avail	100
Print	100
Serial	100

A

REPORT DOCUMENTATION PAGE			READ INSTRUCTIONS BEFORE COMPLETING FORM
1. REPORT NUMBER Final Report	2. GOVT ACCESSION NO. AD-A103 805	3. RECIPIENT'S CATALOG NUMBER	
4. TITLE (and Subtitle) Radar Waveform Synthesis for Target Identification	5. TYPE OF REPORT & PERIOD COVERED Final Report - May 5, 1980 to May 4, 1981		
A088673		6. PERFORMING ORG. REPORT NUMBER	
7. AUTHOR(s) Kun-Mu Chen	7. CONTRACT OR GRANT NUMBER(s) N00019-18-K-0382		
8. PERFORMING ORGANIZATION NAME AND ADDRESS Division of Engineering Research Michigan State University East Lansing, Michigan 48824	10. PROGRAM ELEMENT, PROJECT, TASK AREA & WORK UNIT NUMBERS		
11. CONTROLLING OFFICE NAME AND ADDRESS Naval Air Systems Command Department of the Navy	12. REPORT DATE June 3, 1981		
14. MONITORING AGENCY NAME & ADDRESS (if different from Controlling Office)	13. NUMBER OF PAGES 75		
15. SECURITY CLASS. (of this report) unclassified			
15a. DECLASSIFICATION/DOWNGRADING SCHEDULE			
16. DISTRIBUTION STATEMENT (of this Report) Approved for public release; distribution unlimited.			
17. DISTRIBUTION STATEMENT (of the abstract entered in Block 20, if different from Report) NA			
18. SUPPLEMENTARY NOTES The findings of this report are not to be construed as an official Department of the Navy position, unless so designated by other authorized documents.			
19. KEY WORDS (Continue on reverse side if necessary and identify by block number) Radar signal waveform synthesis, natural resonance mode, arbitrarily oriented thin wire, sphere, infinite cylinder, single-mode backscatter, discrimination of radar targets, incident radar signal, return radar signal			
20. ABSTRACT (Continue on reverse side if necessary and identify by block number) A new scheme for radar detection and discrimination, the radar waveform synthesis method, is investigated. This scheme consists of synthesizing an aspect-independent waveform for the incident radar signal which excites an arbitrarily oriented target in such a way that the return radar signal from the target contains only a single natural resonance mode of the target in the late-time period. When the synthesized incident radar sig-			

unclassified

SECURITY CLASSIFICATION OF THIS PAGE(When Data Entered)

ignal for exciting a particular natural mode of a known, preselected target is applied to a wrong target, the return radar signal will be significantly different from that of the expected natural mode, thus, the wrong target can be sensitively discriminated. The selection of an optimum pulse duration of the required incident signal for the purpose of shaping its waveform is also studied.

Three kinds of targets, an arbitrarily oriented thin wire, a sphere and a normally oriented infinite cylinder, have been investigated. The cases of an arbitrarily oriented wire and a sphere have been completed and the results are reported in Parts 1 and 2. The case of infinite cylinder will be completed shortly and incomplete results of this case are outlined in Part 3.

f

unclassified

SECURITY CLASSIFICATION OF THIS PAGE(When Data Entered)

PART 1

RADAR WAVEFORM SYNTHESIS FOR SINGLE-MODE BACK-
SCATTERING BY AN ARBITRARILY ORIENTED WIRE

1. Introduction

In recent years, research on radar target identification and discrimination utilizing a short-pulse waveform has been conducted by a number of workers [1-8]. One interesting scheme is to irradiate a target with a simple waveform such as an impulse, a step or a ramp signal, and then analyze the scattered field from the target in terms of natural resonance modes of the target. It is known that the waveform of the scattered field is aspect dependent, but the set of natural resonant frequencies extracted from the scattered field is independent of the aspect angle [9-13]. Using this property, a target can be identified if the extracted set of natural frequencies is compared with the collection of known data on the natural frequencies of various targets. Two different targets can also be differentiated if the two sets of natural frequencies are compared. One of the problems associated with this scheme is difficulty in obtaining accurate natural frequencies of the target from a noisy scattered field.

In this paper, an inverse scheme, to be called the radar-waveform-synthesis method, is investigated. Instead of analyzing the field scattered by the target in terms of its natural resonance modes, this new scheme synthesizes the waveform of the incident radar signal in such a way that, when it excites the target, the return radar signal contains only a single natural mode of the target. It will be shown that when the incident radar signal synthesized to excite a particular natural mode of a preselected target is applied to a different target, the return signal will be significantly different from that of the expected natural mode. The wrong target can thus be sensitively discriminated.

The simplest case of this radar waveform synthesis scheme has been studied by Chen [14] for the case of a thin wire irradiated by a radar pulse at normal incidence. For this case, it is possible to synthesize a required waveform for the incident radar wave to excite a single-mode return response at all post-incidence times. When this study is generalized to oblique incidence, difficulties are encountered in obtaining a realizable required incident waveform for exciting a single-mode, scattered field. Furthermore,

the required incident radar signal appears to be aspect dependent. This difficulty arises because there exists a finite transit time for an obliquely-oriented wire, i.e. a finite time for an impulse to pass the wire. The impulse response of this wire consists of an early-time, forced response in addition to the sum of natural modes which describes a normally oriented wire. This early-time, forced impulse response is difficult to approximate analytically, and consequently is responsible for problems encountered when synthesizing an incident radar signal to excite a single-mode, scattered field at all post-incidence times.

To overcome this difficulty, we have concentrated on the behavior of the late-time response of the wire, and have found a scheme to synthesize the required waveform for an incident radar signal of finite duration to excite a single-mode, scattered field in the late-time period (where the early-time impulse response is not required, since that period has elapsed). More significantly, this synthesized incident radar signal was found to be aspect independent.

Initially the impulse response of an obliquely oriented wire is approximated analytically. This response is found to consist of a forced response, which exists only during the early-time period, augmenting a causal sum of natural resonance modes. It is next demonstrated that an aspect-independent, incident radar signal which excites a single-mode return signal after the early-time period can be synthesized. The aspect-independent, required waveforms of the incident radar signals which excite various single-mode return signals from an arbitrarily oriented wire are then obtained. Numerical examples on required waveforms for exciting various single-mode return signals, and those on the return signals from a wire oriented at various angles are given. Numerical examples are also given to show that when the synthesized incident signal which excites a particular natural mode of a preselected target is applied to a different target, the return signal from the wrong target becomes significantly different from that of the expected natural mode. The possibility of shaping the waveform of the required incident signal by adjusting the duration of the

incident signal, and other features of the radar waveform synthesis method are also discussed.

2. Geometry of Problem

A thin-wire cylinder of length L and radius a is illuminated by an incident-wave radar signal at angle θ as indicated in Fig. 1. The electric field of this transient plane wave is assumed to be

$$\vec{E}^i(z, t) = \hat{\zeta} F(t - z \cos \theta / c) \quad (1)$$

where polarization is specified by constant vector $\hat{\zeta}$ and $F(t)$ is an unknown waveform function to be determined by the requirement that $\vec{E}^i(z, t)$ excite a single-mode, scattered field. The component of $\vec{E}^i(z, t)$ tangential to the wire surface, in the Laplace transform domain, is

$$\vec{E}_{\tan}^i(z, s) = \sin \theta F(s) e^{-sz} \cos \theta / c \quad (2)$$

This electric field excites a transient induced current on the wire, and the induced current subsequently generates a transient backscattered electric field. The goal is to synthesize an aspect-independent waveform $F(t)$ for the incident radar signal in such a way that the backscattered field, or the return radar signal, from the wire oriented at any aspect angle θ contains only a single natural mode of the target.

3. Induced Current and Backscattered Field

The induced current, $I(z, s)$, on the wire can be found as the solution to Pocklington's integral equation [10]

$$\int_0^L \Gamma(z, z', s) I(z', s) dz' = S(z, s) \quad (3)$$

with the thin-wire kernel

$$\Gamma(z, z', s) = \left(\frac{\partial^2}{\partial z^2} - \frac{s^2}{c^2} \right) \frac{e^{-sR/c}}{4\pi R}, \quad R = \sqrt{(z-z')^2 + a^2} \quad (4)$$

and the excitation forcing function

$$S(z, s) = -\epsilon_0 \sin\theta [s F(s) e^{-sz} \cos\theta/c]. \quad (5)$$

If the only singularities of $I(z, s)$ in the finite, complex s -plane are simple poles at natural frequencies $s_\alpha = \sigma_\alpha + j\omega_\alpha$ and it is assumed that no entire-function contribution exists, then the SEM representation [9,12] for the induced-current solution to eq. (3) is

$$I(z, s) = \sum_{\alpha=1}^N a_\alpha(s) v_\alpha(z) (s-s_\alpha)^{-1} \quad (6)$$

where $v_\alpha(z)$ is the current distribution of the α th natural-resonance mode. Coupling coefficients $a_\alpha(s)$ are obtained [12] from the inverse operator to integral equation (3) with the "class-2" [9] representation

$$a_\alpha(s) = \frac{\int_0^L s(z, s) v_\alpha(z) dz}{\int_0^L dz v_\alpha(z) \int_0^L v_\alpha(z') \left[\frac{\partial}{\partial s} \Gamma(z, z', s) \right] \Big|_{s=s_\alpha} dz'} \quad (7)$$

A development of this result specific to the thin-wire scatterer is presented in the Appendix; it demonstrates the apparent approximate nature of that representation for $a_\alpha(s)$. Since the above coupling coefficient is frequency dependent, it leads as necessary to an early-time response having a forced component which differs from a pure sum of natural modes. If $v_\alpha(z)$ is represented by the well known approximation

$$v_\alpha(z) = \sin\left(\frac{\alpha\pi z}{L}\right) \quad (8)$$

$a_\alpha(s)$ can be evaluated in closed form, and the induced current $I(z, s)$ is determined to be

$$I(z, s) = \frac{4\pi^2 \sin\theta}{\mu_0 L^2 [2 \log(L/a) - 1]} s F(s) \times$$

$$\sum_{\alpha=1}^N \alpha \left[\frac{1 - (-1)^\alpha e^{-sL \cos\theta/c}}{s^2 \cos^2\theta/c^2 + \alpha^2 \pi^2/c^2} \right] \left[\frac{1}{s_\alpha (s-s_\alpha)} + \frac{1}{s_\alpha^* (s-s_\alpha^*)} \right] \sin\left(\frac{\alpha\pi z}{L}\right).$$

The backscattered electric field can be determined from the far-field expression

$$\vec{E}^s(s) = -\hat{\zeta} s A(s) \sin\theta \quad (10)$$

where $A(s)$ is the vector potential in the backscattered direction maintained by $I(z, s)$, and it can be expressed as

$$A(s) = \frac{\mu_0}{4\pi R_\infty} e^{-sR_\infty/c} \int_0^L I(z, s) e^{-sz \cos\theta/c} dz \quad (11)$$

R_∞ in eq. (11) is the distance between the wire and a distant observation point in the cylinder's radiation zone.

The final expression for $E^s(s)$ can then be obtained as

$$E^s(s) = K_1 \frac{e^{-sR_\infty/c}}{R_\infty} F(s) H(s, \theta) \quad (12)$$

where

$$K_1 = \frac{-L \sin^2\theta}{\pi^2 [2 \log(L/a) - 1]}, \text{ and} \quad (13)$$

$F(s)$ = waveform function of the incident radar signal.
Transfer function $H(s, \theta)$ in eq. (12) is expressed as

$$H(s, \theta) = \sum_{\alpha=1}^N \frac{s^2}{\alpha^2} \left[\frac{1 - (-1)^\alpha e^{-sT}}{1 + (T/\alpha\pi)^2 s^2} \right]^2 \left[\frac{1}{s_\alpha (s-s_\alpha)} + \frac{1}{s_\alpha^* (s-s_\alpha^*)} \right]$$

$$(14)$$

where the incident-wavefront transit time is

$$T = (L/c) \cos\theta. \quad (15)$$

It appears feasible at this point to synthesize $F(s)$ required to excite a single-mode scattered field by requiring $E^s(s)$ to represent such a field in eq. (12) and subsequently solving for $F(s)$ in terms of known $H(s, \theta)$. This procedure was implemented successfully [14] for the special case of normal incidence. With obliquely-incident illumination, it becomes difficult, due to the complex frequency dependence of $H(s, \theta)$, to evaluate $f(t)$ by numerically inverse transforming $F(s)$; furthermore $f(t)$ is a very ill-behaved signal in the early-time period. The latter problem arises because the above synthesis procedure demands that $E^s(t, \theta)$ consist of a single natural mode at all post-incidence times, including the early-time period where the forced impulse response is poorly behaved and difficult to approximate. If the frequency-domain synthesis method is abandoned, then these difficulties are overcome by adopting a time-domain synthesis procedure for incident signals of finite duration T_e . When $E^s(t, \theta)$ is not constrained in the early-time period $0 < t < T_e + 2T$, then the forced impulse response is not encountered and it is found that a single-mode scattered field can be excited in the late-time period $t > T_e + 2T$ by well-behaved, aspect-independent incident waveforms of finite duration.

4. Impulse Response

The impulse response $h(t, \theta)$ of the wire is first determined by inverting the transfer function as

$$h(t, \theta) = L^{-1} [H(s, \theta)] = \sum_{\alpha=1}^N h_{\alpha}(t, \theta). \quad (16)$$

$h(t, \theta)$ is a function of aspect angle θ , and $h_{\alpha}(t, \theta)$ represents that impulse response associated with the α 'th natural mode. It is found that $h_{\alpha}(t, \theta)$ can be obtained analytically in closed form by inversion of $H_{\alpha}(s, \theta)$; it is decomposed into an early-time forced component which is nonzero only for $0 < t < 2T$ and a natural component, consisting of a pure natural mode, which exists for all $0 < t < \infty$. These results are summarized below.

During the early-time period $0 \leq t \leq 2T$ the forced response is

$$h_\alpha(t, \theta) = \frac{\alpha\pi^3}{T^3 |s_\alpha|^2} e^{\sigma_\alpha t} \left[[\sigma_\alpha g_1(t) - \omega_\alpha g_2(t)] \cos \omega_\alpha t + [\omega_\alpha g_1(t) + \sigma_\alpha g_2(t)] \sin \omega_\alpha t \right], \quad (17)$$

while for the late-time period of $t \geq 2T$ the natural response is

$$h_\alpha(t, \theta) = \frac{\alpha\pi^3}{T^3 |s_\alpha|^2} e^{\sigma_\alpha t} \left[[\sigma_\alpha g_1(2T) - \omega_\alpha g_2(2T)] \cos \omega_\alpha t + [\omega_\alpha g_1(2T) + \sigma_\alpha g_2(2T)] \sin \omega_\alpha t \right] \quad (18)$$

where

$$g_1(t) = \int_0^t e^{-\sigma_\alpha t'} \cos \omega_\alpha t' [f_1(t') \sin bt' + bf_2(t') \cos bt'] dt' \quad (19)$$

$$g_2(t) = \int_0^t e^{-\sigma_\alpha t'} \sin \omega_\alpha t' [f_1(t') \sin bt' + bf_2(t') \cos bt'] dt' \quad (20)$$

$$f_1(t) = u(t) - 2u(t-T) + u(t-2T) \quad (21)$$

$$f_2(t) = tu(t) - 2(t-T)u(t-T) + (t-2T)u(t-2T) \quad (22)$$

$$b = \frac{\alpha\pi}{T}, \text{ and } T = (L/c)\cos\theta.$$

If integrals $g_1(t)$ and $g_2(t)$ are calculated, the impulse response is expressed in an alternative form as

$$\begin{aligned}
 h_\alpha(t, \theta) = & [u(t) G_\alpha(t) - 2(-1)^\alpha u(t-T) G_\alpha(t-T) + u(t-2T) G_\alpha(t-2T)] \\
 & - 2[B_{\alpha r}(s_\alpha) f_1(t) - C_{\alpha r}(s_\alpha) f_2(t)] \sin bt \\
 & - 2[D_{\alpha r}(s_\alpha) f_1(t) + E_{\alpha r}(s_\alpha) f_2(t)] \cos bt \quad (23)
 \end{aligned}$$

where

$$G_\alpha(t) = 2e^{\sigma_\alpha t} [A_{\alpha r}(s_\alpha) \cos \omega_\alpha t - A_{\alpha i}(s_\alpha) \sin \omega_\alpha t] \quad (24)$$

$$A_\alpha(s_\alpha) = \frac{b^4 s_\alpha}{\alpha^2 (s_\alpha^2 + b^2)^2}, \quad B_\alpha(s_\alpha) = \frac{b^3 (s_\alpha^2 - b^2)}{2\alpha^2 (s_\alpha^2 + b^2)^2}$$

$$C_\alpha(s_\alpha) = \frac{b^5}{2\alpha^2 s_\alpha (s_\alpha^2 + b^2)}, \quad D_\alpha(s_\alpha) = \frac{b^4 s_\alpha}{\alpha^2 (s_\alpha^2 + b^2)^2}$$

$$E_\alpha(s_\alpha) = \frac{b^4}{2\alpha^2 (s_\alpha^2 + b^2)}$$

With $B_{\alpha r}(s_\alpha) = \text{Re}\{B_\alpha(s_\alpha)\}$, etc. The first term of eq. (23) is a natural mode and the second and third terms represent a forced response which exists only during the period of $0 \leq t \leq 2T$ where $T=L \cos \theta/c$. Thus, the impulse response, $h(t, \theta)$, consists of a natural component which is the sum of natural modes and exists for all times, and a forced component which exists only in the early-time period of $0 \leq t \leq 2T$.

Impulse-response waveforms for the thin-cylinder structure are indicated in Figs. 2 and 3. Fig. 2 displays the impulse responses obtained by summing the first 10 natural modes (first layer of poles) in series (16) for 60° and 30° aspect angles. The impulse response is observed to depend strongly upon the aspect angle and to consist of a rapidly-oscillating forced response during the early-time period $0 \leq t \leq 2T$ followed by the relatively-slowly-varying natural response (a sum of pure natural modes) in the late-time period $2T \leq t < \infty$. Convergence of the impulse-response series was checked at 60° aspect by including 999 terms (pole lo-

cations estimated by an approximate recursion method) with results as indicated in Fig. 3. The result is observed to be a smoothing of the late-time response, which is well approximated by the 10-term series, while the rapidly-oscillating, early-time response persists with increased frequency. Further convergence studies indicated that the second and third layers of poles provide essentially no contribution to the late-time natural response, while their early-time nature is also rapidly oscillatory and does not result in smoothing the total early-time impulse response. Although adequate convergence of the early-time impulse response could not be achieved (this may be related to a Gibb's-type phenomenon), it is noted that convolution of this response with any relatively-smooth signal, e.g., a step or a Gaussian pulse, will eliminate the rapid oscillation leaving essentially the envelope of that response. The latter results are similar to step and smoothed-impulse responses obtained by other investigators.

The difficulty encountered during initial attempts to synthesize an incident waveform which excites a single-mode scattered field at all post-incidence times is due to the erratic behavior of the approximated forced impulse response during its early-time period. If the scatter-field waveform, given by the convolution $E^S(t, \theta) = f(t) * h(t, \theta)$, is required to consist of a single natural mode for all $t > 0$, then required incident signal $f(t)$ must be such as to smooth the early-time forced impulse response which is intersected in the convolution; the result is a poorly-behaved required incident waveform. To overcome this difficulty, a time-domain synthesis procedure for incident waveforms of finite duration T_e is developed which requires single-natural-mode scatter field response in the late-time period $t > T_e + 2T$ but does not constrain that response in the early-time period $0 < t < T_e + 2T$. It is emphasized that this method avoids the forced impulse response entirely, such that this slowly-convergent component is never required.

5. Single-Mode Excitation

It was demonstrated in eq. (23) that the impulse response can be expressed as

$$h(t, \theta) = \xi(t, \theta) + \sum_{n=1}^N a_n(\theta) e^{\sigma_n t} \cos(\omega_n t + \phi_n(\theta)) \quad (25)$$

where

$\xi(t, \theta)$ = forced response which exists only during the period of $0 \leq t \leq 2T$,

$\sum_{n=1}^N a_n(\theta) e^{\sigma_n t} \cos(\omega_n t + \phi_n(\theta))$ = the sum of natural modes which exists for all t ,

$a_n(\theta)$ = aspect dependent amplitude of the n th natural mode,

$\phi_n(\theta)$ = aspect dependent phase angle of the n th natural mode,

and $\sigma_n + j\omega_n = s_n$ = the n th natural frequency. $h(t, \theta)$ is shown graphically in fig. 4a.

If the wire is illuminated with an incident signal, $E^i(t)$, of duration T_e as shown in fig. 4b, the scattered field, $E^s(t)$, should appear like that shown in fig. 4c, consisting of an irregular waveform for the early-time period $0 \leq t \leq T_e + 2T$ followed by a pure single natural mode for $t \geq T_e + 2T$ if the waveform of $E^i(t)$ is properly synthesized. This phenomenon can be shown mathematically as follows.

The scattered field, $E^s(t, \theta)$, can be expressed, based on the convolution theorem, as

$$\begin{aligned} E^s(t, \theta) &= \int_0^{T_e} E^i(t') h(t-t', \theta) dt' \\ &= \int_0^{T_e} E^i(t') \left[\xi(t-t', \theta) + \sum_{n=1}^N a_n(\theta) e^{\sigma_n(t-t')} \right. \\ &\quad \left. \cdot \cos(\omega_n(t-t') + \phi_n(\theta)) \right] dt' . \end{aligned}$$

For the late time period $t \geq T_e + 2T$, the forced response term does not contribute to the integral because $\xi(t-t', \theta) = 0$ for $0 \leq t' \leq T_e$ if $t \geq T_e + 2T$. The property $\xi(t, \theta) = 0$ for $t \geq 2T$ has been used. The scattered field in the late-time period then becomes

$$E^s(t, \theta) = \int_0^{T_e} E^i(t') \left[\sum_{n=1}^N a_n(\theta) e^{\sigma_n(t-t')} \cos[\omega_n(t-t') + \phi_n(\theta)] \right] dt' \quad \dots \text{ for } t \geq T_e + 2T. \quad (26)$$

Equation (26) can be rewritten as

$$E^s(t, \theta) = \sum_{n=1}^N a_n(\theta) e^{\sigma_n t} [A_n \cos(\omega_n t + \phi_n(\theta)) + B_n \sin(\omega_n t + \phi_n(\theta))] \quad (27)$$

where the coefficients A_n and B_n are defined as

$$\begin{Bmatrix} A_n \\ B_n \end{Bmatrix} = \int_0^{T_e} E^i(t') e^{-\sigma_n t'} \begin{Bmatrix} \cos \omega_n t' \\ \sin \omega_n t' \end{Bmatrix} dt'. \quad (28)$$

It is important to observe that A_n and B_n are independent of the aspect angle θ . It is possible to choose an optimal $E^i(t)$ in such a way that all the coefficients vanish except one; by so doing, $E^s(t, \theta)$ will consist of a single natural mode.

6. Required Incident Signals and Return Signals

It is possible to choose an aspect-independent $E^i(t)$ to excite a single-mode $E^s(t, \theta)$. Consider initially the class of incident

waveforms $E^i(t)$ constructed as a linear combination of natural modes (this choice is generalized in Sect. 9) as

$$E^i(t) = \sum_{m=1}^N e^{\sigma_m t} (b_m \cos \omega_m t + c_m \sin \omega_m t) \quad (29)$$

where $s_m = \sigma_m + j\omega_m$ is the m 'th natural frequency, and b_m and c_m are unknown coefficients to be determined based on the requirement that only a single-mode $E^s(t, \theta)$ be excited.

Substituting representation (29) in eq. (28) leads to

$$A_n = \sum_{m=1}^N M_{nm}^1 b_m + \sum_{m=1}^N M_{nm}^2 c_m \quad (30)$$

$$B_n = \sum_{m=1}^N M_{nm}^3 b_m + \sum_{m=1}^N M_{nm}^4 c_m \quad (31)$$

where

$$\left\{ \begin{array}{l} M_{nm}^1 \\ M_{nm}^2 \\ M_{nm}^3 \\ M_{nm}^4 \end{array} \right\} = \int_0^{T_e} e^{-(\sigma_n - \sigma_m)t'} \left\{ \begin{array}{l} \cos \omega_n t' \cos \omega_m t' \\ \cos \omega_n t' \sin \omega_m t' \\ \sin \omega_n t' \cos \omega_m t' \\ \sin \omega_n t' \sin \omega_m t' \end{array} \right\} dt' \quad (32)$$

It is observed that the M_{nm}^i 's are explicit functions of incident radar pulse duration T_e , and T_e is a parameter of freedom which can be varied to obtain a desirable $E^i(t)$ waveform.

The unknown coefficients b_m and c_m can be solved for from eqs. (30) and (31) as

$$\begin{bmatrix} b_1 \\ b_2 \\ \vdots \\ b_N \\ \hline c_1 \\ c_2 \\ \vdots \\ c_N \end{bmatrix} = \begin{bmatrix} M_{nm}^1 & & M_{nm}^2 \\ & \ddots & \\ & & M_{nm}^3 & M_{nm}^4 \end{bmatrix}^{-1} \begin{bmatrix} A_1 \\ A_2 \\ \vdots \\ A_N \\ \hline B_1 \\ B_2 \\ \vdots \\ B_N \end{bmatrix} \quad (33)$$

In eq. (33), matrix $[M_{nm}]$ is of $2N \times 2N$ order, while $[b_i]$ and $[A_i]$ are two column $2N$ matrices.

To obtain a single-mode scattered field (e.g. the j 'th mode), it is required that $B_j=1$ and $B_n=0$ for $n \neq j$ and $A_n=0$ for all n . b_m and c_m are easily determined from eq. (33), and $E^i(t)$ is subsequently obtained from representation (29). With this $E^i(t)$, the scattered field, $E^s(t, \theta)$, will be

$$E^s(t, \theta) = a_j(\theta) e^{\sigma_j t} \sin(\omega_j t + \phi_j(\theta)) \quad (34)$$

It is noted that with this synthesized $E^i(t)$, the scattered field, $E^s(t, \theta)$, remains single-mode for any aspect angle θ , even though the amplitude $a_j(\theta)$ and the phase angle $\phi_j(\theta)$ vary with θ . In other words, when this synthesized $E^i(t)$ illuminates the wire, the return signal contains only a single natural mode for any aspect angle of the wire.

Numerical results computed according to this scheme are shown in figs. 5 to 10. It was found that when the duration of the incident signal, T_e , is one period of the first natural mode, the required incident signal also becomes predominantly single-mode. That is

$$T_e = T_1 = \frac{1}{f_1} = \frac{2\pi}{\omega_1} = \frac{2\pi}{0.9251(\pi c/L)} = 2.16 \left(\frac{L}{c}\right)$$

leads to a desirable waveform for the incident signal. Fig. 5 shows the required waveforms for the incident radar signal to excite a return radar signal from an arbitrarily oriented wire containing only the first, the second and the third natural mode, respectively. For the first-mode excitation, the required incident signal consists of one cycle of the first natural mode and some small components of higher-order modes as shown in fig. 5a. For the second-mode excitation, the required incident signal consists of about two cycles of the second natural mode and some small components of other modes as shown in fig. 5b. This required waveform looks like a distorted second natural mode. For the third-mode excitation, the required incident signal consists mainly of about three cycles of the third natural mode as shown in fig. 5c. It is emphasized that these required waveforms are independent of aspect angle, or valid for any aspect angle of the wire.

Fig. 6 shows the return radar signals from a wire oriented at various angles, $\theta=15^\circ, 45^\circ, 60^\circ$ and 89° , when the wire is illuminated by the incident radar signal of fig. 5a which is synthesized for the first-mode excitation. It is observed that the return signal for each case of aspect angle remains that of the first natural mode, even though the amplitude and the phase angle vary with the aspect angle. Also the late-time period starts at different time for different aspect angles. These changes in the amplitude, the phase angle, and the starting point of the late-time period with the change in the aspect angle are not important in the practical detection of the return signal; the most important and desirable feature of the return signal is for it to remain single-mode. A single-mode, return signal can be easily identified if it is displayed visually. It is noted that the return signal during the early-time period changes irregularly with the aspect angle, and it is not shown in the figure for the sake of clarity.

Fig. 7 shows the return radar signals from a wire oriented at various angles of $15^\circ, 45^\circ, 60^\circ$ and 89° , when the wire is

illuminated by the incident radar signal of Fig. 5c which is synthesized for the third-mode excitation. Again, the return signal remains that of the third natural mode for any aspect angle.

7. Target Discrimination

When the synthesized incident signal for exciting a particular natural mode of a particular target is applied to a different target, the return signal from the wrong target is expected to be significantly different from that of a single natural mode. Thus, the wrong target can be sensitively discriminated. Two numerical examples are given.

Fig. 9 shows the return radar signals from three targets, the right target (wire), a wire 5% longer than the right target and a wire 20% longer, when they are illuminated at 30° aspect angle by the incident radar signal of fig. 5a which is synthesized for exciting the first natural mode of the right target. It is observed in fig. 9 that the return radar signal from the right target is a pure first natural mode; that from the 5% longer target displays a slightly distorted waveform and a shifted frequency from that of the first natural mode of the right target; and that from the 20% longer target shows an irregular waveform. Based on these return signals, it is easy to discriminate the wrong targets from the right target.

Figure 10 shows the return radar signals from the same three targets of fig. 9 when they are illuminated at 60° aspect angle by the incident radar signal of fig. 5c which is synthesized for exciting the third natural mode of the right target. The return radar signal from the right target shows a pure third natural mode, that from the 5% longer target displays an irregular amplitude variation and a shifted frequency, and that from the 20% longer target shows an irregular waveform. Again, the wrong targets can be easily discriminated from the right target.

8. Pulse Duration and Waveform of Required Incident Signal

In Section 6, it was indicated that the waveform of the

required incident signal for exciting a single-mode return signal can be controlled by adjusting the pulse duration, T_e , of the incident signal. Through extensive numerical calculation, it was found that when T_e is equal to or greater than T_1 , the period of the first natural mode, the aspect-independent, required incident signal for exciting a single-mode return signal consists mainly of that wanted natural mode, as shown in fig. 5. However, when T_e is less than T_1 , the required incident signal starts to have an irregular waveform and a high amplitude. This phenomenon can be observed in fig. 11, where six waveforms for the aspect-independent, required incident signal for exciting the first natural-mode return signal from an arbitrarily oriented wire are shown for signals possessing six different durations, $T_e = 0.25 T_1$, $0.5 T_1$, $0.75 T_1$, T_1 , $1.5 T_1$, and $2 T_1$. It is observed that for the first three cases, $T_e < T_1$, the waveforms of the required incident signal are radidly oscillatory and of high amplitude, while the last three cases $T_e > T_1$, have quite realizable waveforms of mainly single mode. It is noted that to eliminate any possibility of creating irregular waveforms for the cases of $T_e < T_1$, due to numerical error, the required incident signal for the case of $T_e = 0.5 T_1$ was convolved with the impulse response of the wire, and the numerical result on the return signal turned out to be a pure first natural mode of the wire.

With this example, it is easy to conclude that the optimum pulse duration for the incident signal should be a period of the first natural mode or longer. However, it is found that with an incident signal of longer pulse duration the sensitivity of discrimination between different targets decreases. This is easily visualized because as the pulse duration of the incident signal is increased, the situation approaches to the case of the continuous wave excitation of the target and the return signal will contain only the excitation frequency.

Therefore, in the selection of an optimum pulse duration for the incident signal the following three factors should be considered: (1) the pulse duration should be equal to or longer than a period of the first natural mode of the target, (2) an incident signal of

longer pulse duration may be implemented with less difficulty, and (3) the sensitivity of target discrimination decreases with the increase in the pulse duration.

9. Uniqueness of Synthesized Waveforms

The uniqueness of incident field waveform $E^i(t)$, synthesized to excite a backscattered field consisting of a single natural mode, is considered here. It was demonstrated in the last section that E^i depends strongly upon its duration T_e , so the question of uniqueness must be considered for that class of waveforms with T_e specified. Numerical results in Sections 6-8 are all based upon the natural-mode expansion (29) for $E^i(t)$ with $N=10$ (N = number of terms retained in impulse-response series). Eq. (28) provides $2N$ linear, algebraic equations for the $2N$ amplitude coefficients in the series representation of E^i . For finite N , this solution requires the backscatter field to consist of the single $n=j$ mode, while those modes having $1 \leq n < j$, $j < n \leq N$ are not excited. Modes having $n > N$ are not constrained; this truncation is justified by the negligible contribution of such modes to the late-time impulse response. The question naturally arises whether a different choice of basis functions in the expansion for $E^i(t)$ will lead to the same synthesized waveform. It is conjectured that E^i is unique among the class of waveforms expanded in a complete basis set (the natural modes are believed to be complete, although they are not orthogonal) for N infinite. In practice, N can be truncated at some finite value if the series converge adequately rapidly.

The dependence of E^i upon basis functions in its expansion with $N=10$ was studied using rectangular pulse, impulse, and pure sinusoidal basis functions. Figure 12 indicates results for $E^i(t)$ synthesized to excite a single mode ($n=1$) backscatter field and constructed from the various basis functions. The signal duration was chosen as $T_e = T_1$, and it is observed that E^i obtained with each alternative basis set is similar to the result of the natural-mode expansion.

Each of these $E^i(t)$ waveforms will excite the same $n=1$ mode backscattered field, but will not excite those modes with $1 < n \leq 10$. These E^i waveforms may excite different higher-order modes with $n > 10$, which have not been constrained. As N is increased, the $E^i(t)$ waveforms obtained with different basis sets become more nearly equal, and in the limit $N \rightarrow \infty$ provide a unique representation for E^i .

10. Conclusion

It has been demonstrated that an aspect-independent, optimal incident radar waveform E^i of finite duration T_e can be synthesized to excite a thin-cylinder-target backscatter field which consists of a single natural mode of that target in the late-time period $t > T_e + 2T$ (T = target transit time). By constraining only the late-time target response, a time-domain synthesis technique was developed which does not require knowledge of the forced, early-time impulse response. The optimal signal duration was found to be near $T_e = T_1$ (T_1 = period of first target natural-resonance mode), in which case the E^i waveform is very nearly equal to that of the desired single-natural-mode return signal. Incident signals of shorter duration become poorly behaved with rapid, high-amplitude oscillations, while long duration signals will result in loss of target resolution ability. It was demonstrated that a target-identification scheme based upon illuminating the target with a waveform synthesized to excite a single natural-resonance mode backscatter is capable of sensitive target discrimination, since the response of a wrong target with 5% length deviation differs identifiably from a single-mode signal. Since the narrow-band spectral content of optimal incident waveforms very nearly overlaps that of the response they excite, then this target identification technique should possess inherently good signal-to-noise ratio characteristics, as well as enabling the use of narrow-band filters and amplifiers. Optimal, synthesized incident waveforms of specified, finite duration are unique when represented by expansions in complete basis sets in the limit where all terms in the impulse-response series are included.

Appendix: Mode Amplitude of Induced Current, $a_\alpha(s)$ — Derivation of Eq. (7).

The time dependent amplitudes of the resonant mode for the induced current, $a_\alpha(s)$, as expressed in eq. (7) is derived here.

The substitution of eq. (6) in eq. (3) leads to

$$\sum_{\alpha=1}^N a_\alpha(s) (s-s_\alpha)^{-1} \int_0^L \Gamma(z, z', s) v_\alpha(z') dz' \approx S(z, s) \quad (A1)$$

Defining $\int_0^L \Gamma(z, z', s) v_\alpha(z') dz' \equiv M_\alpha(z, s)$ (A2)

we can rewrite eq. (A1) as

$$\sum_{\alpha=1}^N a_\alpha(s) (s-s_\alpha)^{-1} M_\alpha(z, s) = S(z, s) \quad (A3)$$

Multiplying eq. (A3) with $v_\beta(z)$ and then integrate it over z from 0 to L :

$$\sum_{\alpha=1}^N a_\alpha(s) (s-s_\alpha)^{-1} \int_0^L M_\alpha(z, s) v_\beta(z) dz = \int_0^L S(z, s) v_\beta(z) dz \quad (A4)$$

After defining

$$\int_0^L M_\alpha(z, s) v_\beta(z) dz \equiv M_{\beta\alpha}(s) \quad (A5)$$

and

$$\int_0^L S(z, s) v_\beta(z) dz \equiv S_\beta(s), \quad (A6)$$

we can rewrite eq. (A4) as

$$\sum_{\alpha=1}^N a_\alpha(s) (s-s_\alpha)^{-1} M_{\beta\alpha}(s) = S_\beta(s) \quad (A7)$$

Equation (A7) can be rearranged as

$$a_\beta(s) (s-s_\beta)^{-1} M_{\beta\beta}(s) + \sum_{\substack{\alpha=1 \\ \alpha \neq \beta}}^N a_\alpha(s) (s-s_\alpha)^{-1} M_{\beta\alpha}(s) = S_\beta(s) \quad (A8)$$

The L.H.S. of eq. (A8) appears to have singularities in the s -plane at s_α, s_β, \dots , while the R.H.S. of the equation is analytic. To clear this difficulty, let's expand $M_{\beta\beta}(s)$ and $M_{\beta\alpha}(s)$ into Taylor series' around the respective poles.

$$M_{\beta\beta}(s) = \left[M_{\beta\beta}(s) \right]_{s=s_\beta} + (s-s_\beta) \left[\frac{\partial}{\partial s} M_{\beta\beta}(s) \right]_{s=s_\beta} + \frac{1}{2} (s-s_\beta)^2 \left[\frac{\partial^2}{\partial s^2} M_{\beta\beta}(s) \right]_{s=s_\beta} + \dots \quad (A9)$$

where

$$\left[M_{\beta\beta}(s) \right]_{s=s_\beta} = \int_0^L v_\beta(z) dz \left[\int_0^L \Gamma(z, z', s_\beta) v_\beta(z') dz' \right] = 0 \quad (A10)$$

because if $v_\beta(z')$ is the β th natural mode, no excitation is needed to excite it, and $v_\beta(z')$ should satisfy eq. (3) with $S(z, s)=0$.

$$\begin{aligned} \left[\frac{\partial}{\partial s} M_{\beta\beta}(s) \right]_{s=s_\beta} &= \int_0^L v_\beta(z) dz \left[\int_0^L \left[\frac{\partial}{\partial s} \Gamma(z, z', s) \right]_{s=s_\beta} v_\beta(z') dz' \right] \\ \left[\frac{\partial^2}{\partial s^2} M_{\beta\beta}(s) \right]_{s=s_\beta} &= \int_0^L v_\beta(z) dz \left[\int_0^L \left[\frac{\partial^2}{\partial s^2} \Gamma(z, z', s) \right]_{s=s_\beta} v_\beta(z') dz' \right] \end{aligned} \quad (A11)$$

(A12)

Thus, eq. (A9) becomes

$$M_{\beta\beta}(s) = (s-s_\beta) \left[\frac{\partial}{\partial s} M_{\beta\beta}(s) \right]_{s=s_\beta} + \frac{1}{2} (s-s_\beta)^2 \left[\frac{\partial^2}{\partial s^2} M_{\beta\beta}(s) \right]_{s=s_\beta} + \dots \quad (A13)$$

By expanding $M_{\beta\alpha}(s)$ around $s=s_\alpha$, we can similarly show that

$$M_{\beta\alpha}(s) = (s-s_\alpha) \left[\frac{\partial}{\partial s} M_{\beta\alpha}(s) \right]_{s=s_\alpha} + \frac{1}{2} (s-s_\alpha)^2 \left[\frac{\partial^2}{\partial s^2} M_{\beta\alpha}(s) \right]_{s=s_\alpha} + \dots \quad (A14)$$

If we assume that

$$v_\alpha(z') = \sin \left(\frac{\alpha \pi z'}{L} \right), \quad (A15)$$

we can show after a tedious integration that

$$\int_0^L \left[\frac{\partial}{\partial s} \Gamma(z, z', s) \right]_{s=s_\alpha} v_\alpha(z') dz' \doteq K v_\alpha(z) \quad (A16)$$

where K is a constant. We can then show that

$$\begin{aligned} \left[\frac{\partial}{\partial s} M_{\beta\alpha}(s) \right]_{s=s_\alpha} &= \int_0^L v_\beta(z) dz \left[\int_0^L \left[\frac{\partial}{\partial s} \Gamma(z, z', s) \right]_{s=s_\alpha} v_\alpha(z') dz' \right] \\ &= K \int_0^L v_\beta(z) v_\alpha(z) dz = 0 \quad \text{for } \alpha \neq \beta \end{aligned} \quad (A17)$$

Similarly, we can approximate

$$\left[\frac{\partial^2}{\partial s^2} M_{\beta\alpha}(s) \right]_{s=s_\alpha} \doteq 0 \quad \text{for } \alpha \neq \beta \quad (A18)$$

Thus,

$$M_{\beta\alpha}(s) \doteq 0 \quad \text{if } \alpha \neq \beta \quad (A19)$$

Equation (A8) can now be simplified to

$$a_\beta(s) \left\{ \left[\frac{\partial}{\partial s} M_{\beta\beta}(s) \right]_{s=s_\beta} + \frac{1}{2} (s-s_\beta) \left[\frac{\partial^2}{\partial s^2} M_{\beta\beta}(s) \right]_{s=s_\beta} + \dots \right\} = S_\beta(s) \quad (A20)$$

The first term of the L.H.S. of eq. (A20) usually dominates, especially near $s=s_\beta$. Therefore, $a_\beta(s)$ can be approximately determined as

$$a_\beta(s) = \frac{s_\beta(s)}{\left[\frac{\partial}{\partial s} M_{\beta\beta}(s) \right]_{s=s_\beta}} = \frac{\int_0^L s(z, s) v_\beta(z) dz}{\int_0^L v_\beta(z) dz \left[\int_0^L \left[\frac{\partial}{\partial s} \Gamma(z, z', s) \right]_{s=s_\beta} v_\beta(z') dz' \right]} \quad (A21)$$

which is the result of eq. (7).

REFERENCES

- (1) E. K. Kennaugh and D. L. Moffatt, "Transient and impulse response approximation," Proc. of IEEE, Vol. 53, pp. 893-901, August 1965.
- (2) D. L. Moffatt and R. K. Mains, "Detection and discrimination of radar targets," IEEE Trans. on Ant. and Prop., Vol. AP-23, No. 3, pp. 358-367, May 1975.
- (3) A. J. Berni, "Target identification by natural resonance estimation," IEEE Trans. on Aerospace and Electronic Systems, Vol. AES-11, No. 2, pp. 147-154, March 1975.
- (4) J. D. Young, "Radar imaging from ramp response signatures," IEEE Trans. on Ant. and Prop., Vol. AP-24, No. 3, pp. 276-282, May 1976.
- (5) K. A. Shubert, J. D. Young and D. L. Moffatt, "Synthetic radar imagery," IEEE Trans. on Ant. and Prop., Vol. AP-25, No. 4, pp. 477-483, July 1977.
- (6) C. L. Bennett, W. Weeks, "A technique for computing approximate electromagnetic impulse response of conducting bodies," Purdue University, Lafayette, Indiana, Tech. Report TR-EE68-11, 1968.
- (7) A. G. Repjar, A. A. Ksienki and L. J. White, "Object identification from multi-frequency radar returns," The Radio and Electronics Engineers, Vol. 45, No. 4, pp. 161-167, April 1975.
- (8) C. W. Chuang and D. L. Moffatt, "Natural resonance of radar target via Prony's method and target discrimination," IEEE Trans. on Aerospace and Electronic Systems, Vol. AES-12, No. 5, pp. 583-589.
- (9) C. E. Baum, "Toward an engineering theory of electromagnetic scattering: The singularity and eigenmode expansion methods," in Electromagnetic Scattering, Editor: P.L.E. Uslenghi, Academic Press, New York, 1978, pp. 571-651.
- (10) F. M. Tesche, "On the analysis of scattering and antenna problems using the singularity expansion techniques," IEEE Trans. on Ant. and Prop., Vol. AP-21, No. 1, pp. 53-62, January 1973.
- (11) L. Marin, "Natural-mode representation of transient scattered fields," IEEE Trans. on Ant. Prop., Vol. AP-21, No. 6, pp. 809-818, Nov. 1973.
- (12) L. Marin, "Natural-mode representation of transient scattering from rotationally symmetric bodies," IEEE Trans. on Ant. and Prop., Vol. AP-22, No. 2, pp. 266-274, March 1974.

- (13) M. L. Van Blaricum and R. Mittra, "A technique for extracting the poles and residues of a system directly from its transient response," IEEE Trans. on Ant. and Prop., Vol. AP-23, No. 6, pp. 777-781, November 1975.
- (14) K. M. Chen, "Radar waveform synthesis method--a new radar detection scheme," Presented at 1980 International IEEE/APS Symposium and 1980 National radio science meeting, Quebec City, Canada, June 2-6, 1980.

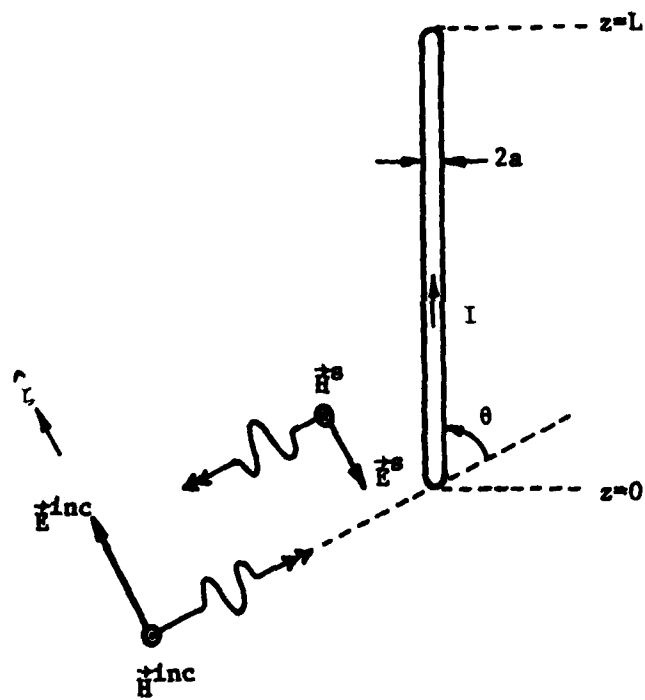


fig. 1. A thin wire is illuminated by a radar signal at an oblique angle.

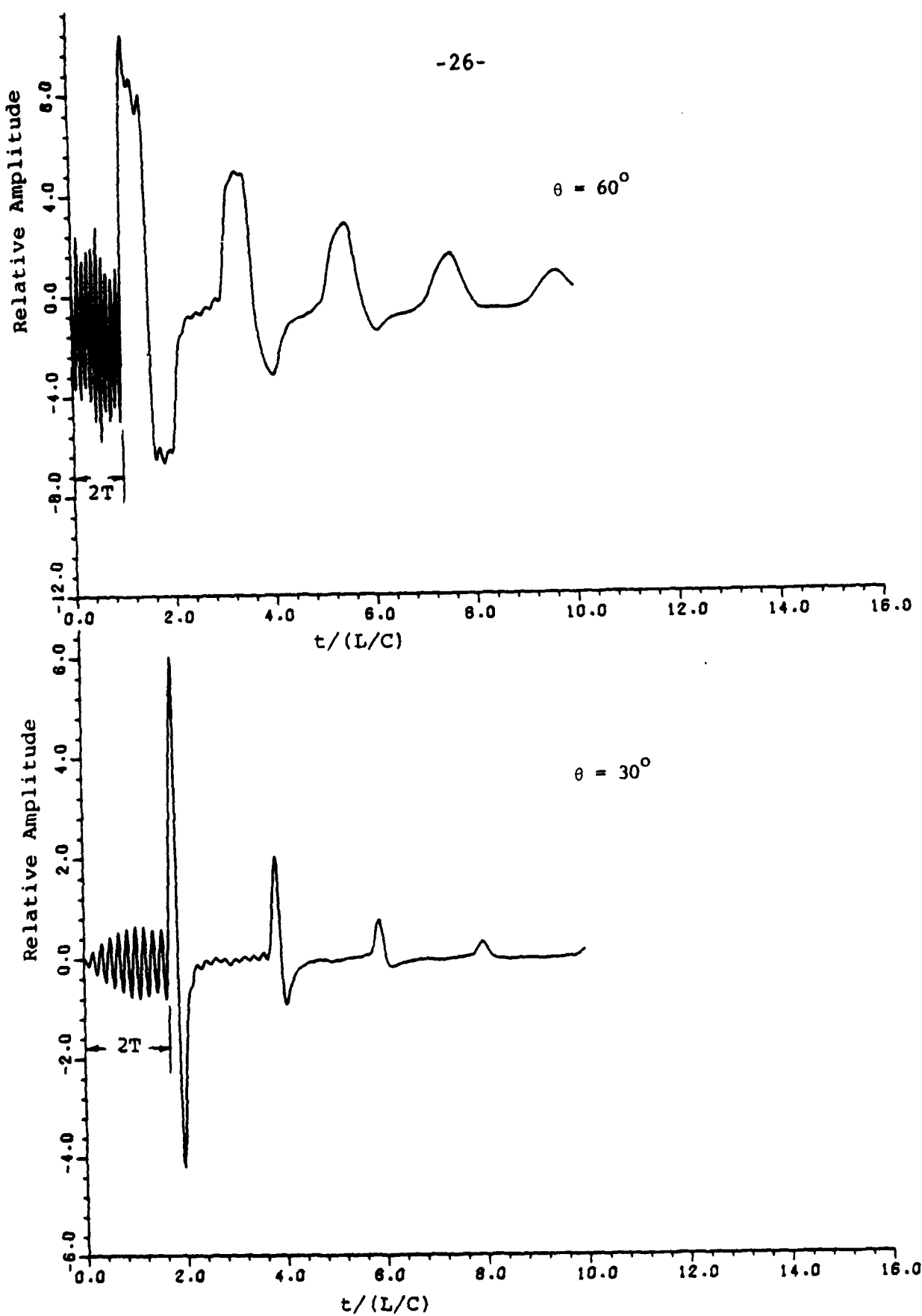


fig. 2. The impulse responses from a wire with 30° and 60° aspect angles ($L/a = 200$).

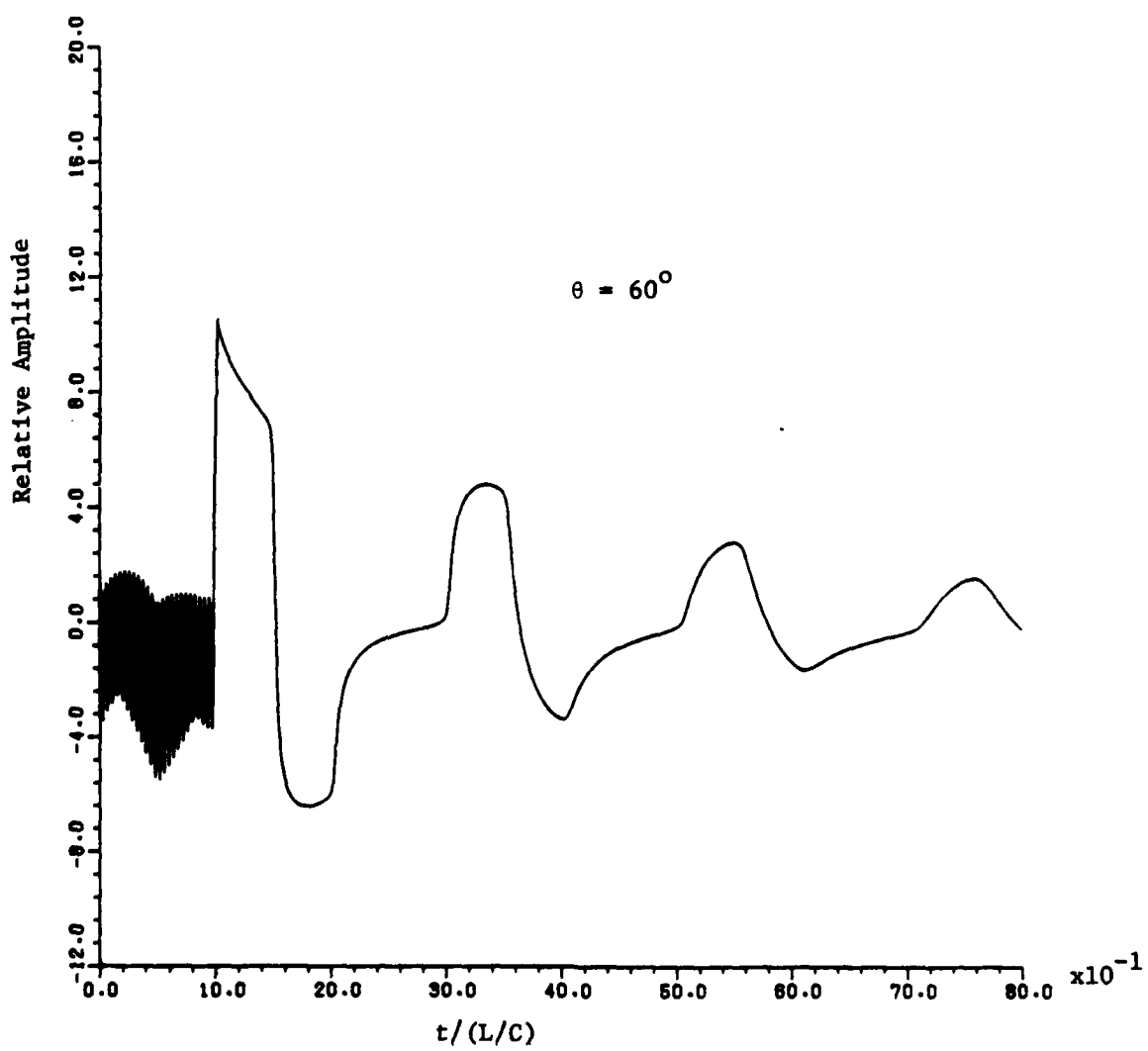


fig. 3. The impulse response from a wire with 60° aspect angle and $L/a = 200$. This impulse response is constructed with 999 natural modes of the wire.

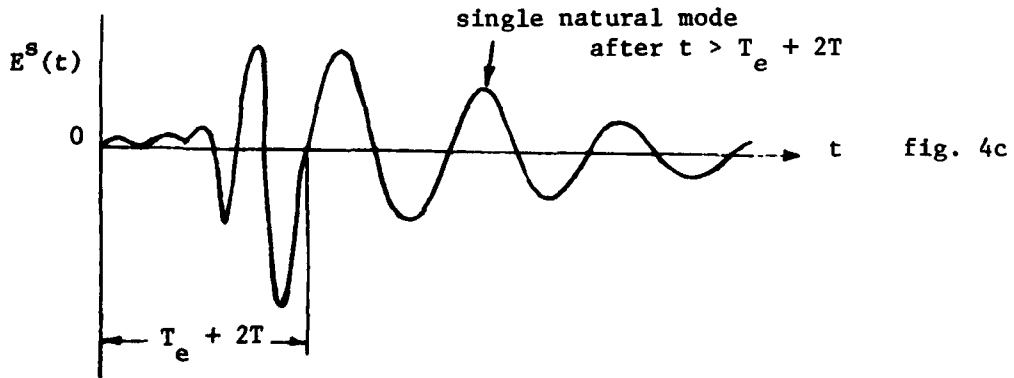
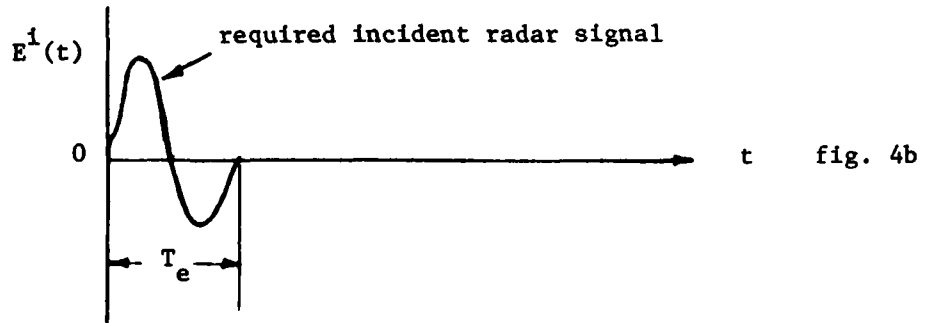
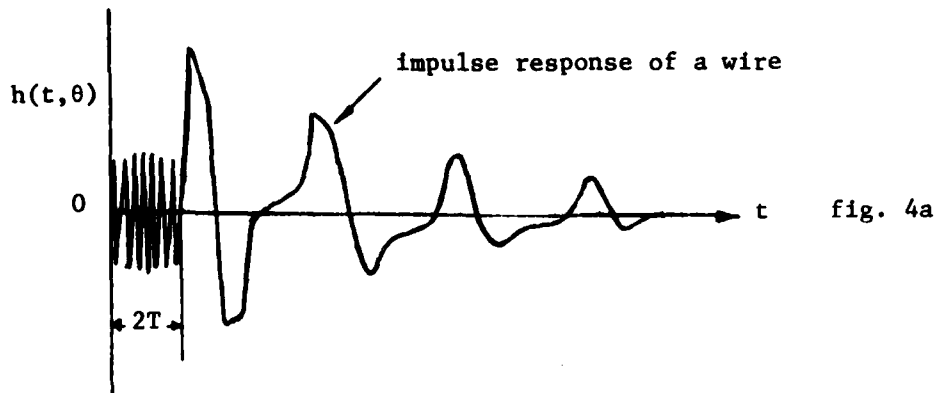


fig. 4. Waveforms of the impulse response of a wire, the required incident signal and the return signal with a single natural mode in the late-time period.

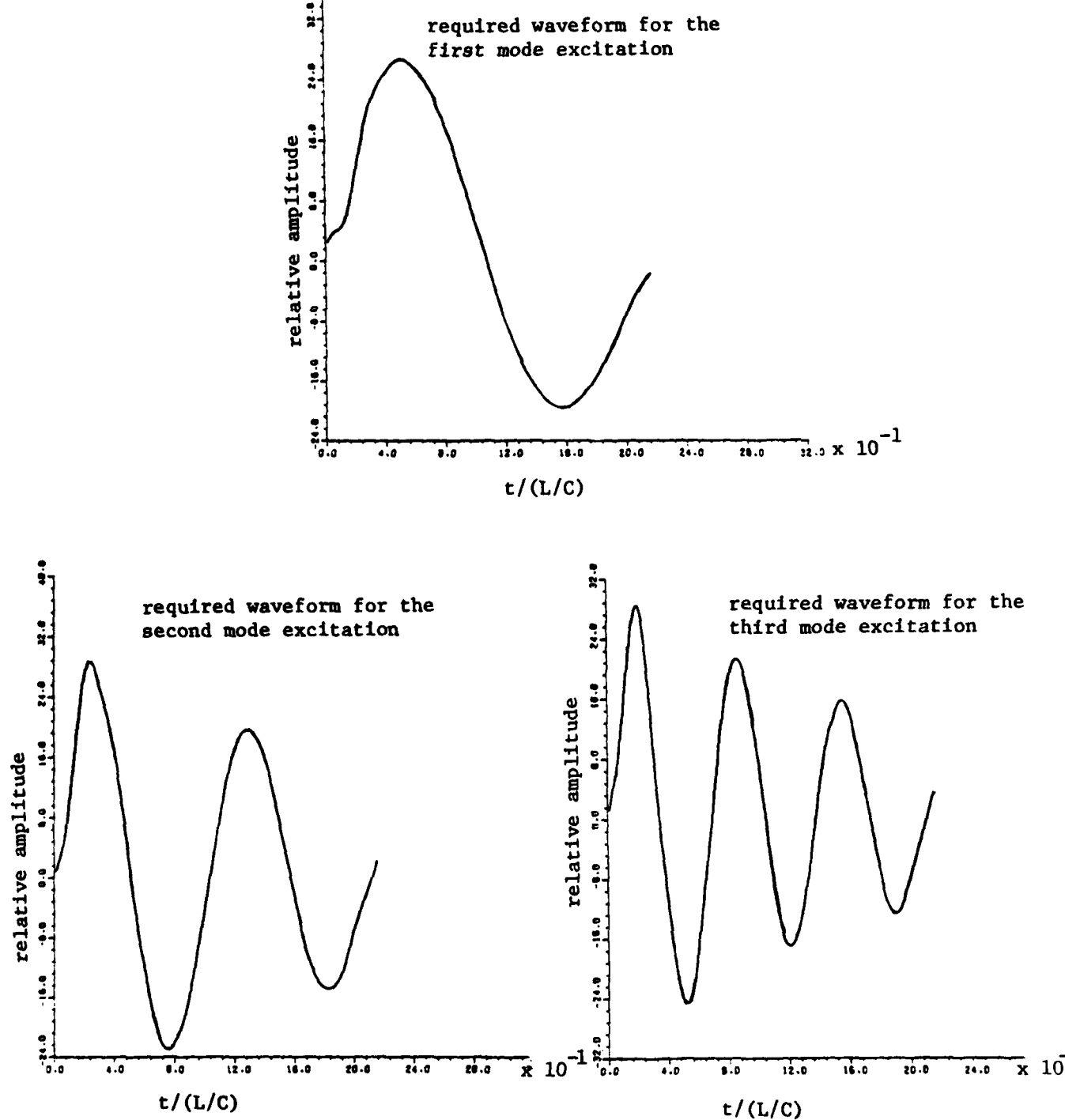


fig. 5. Required waveforms for the incident radar signal to excite a return radar signal from an arbitrarily oriented wire containing only the first, the second and the third natural mode, respectively.

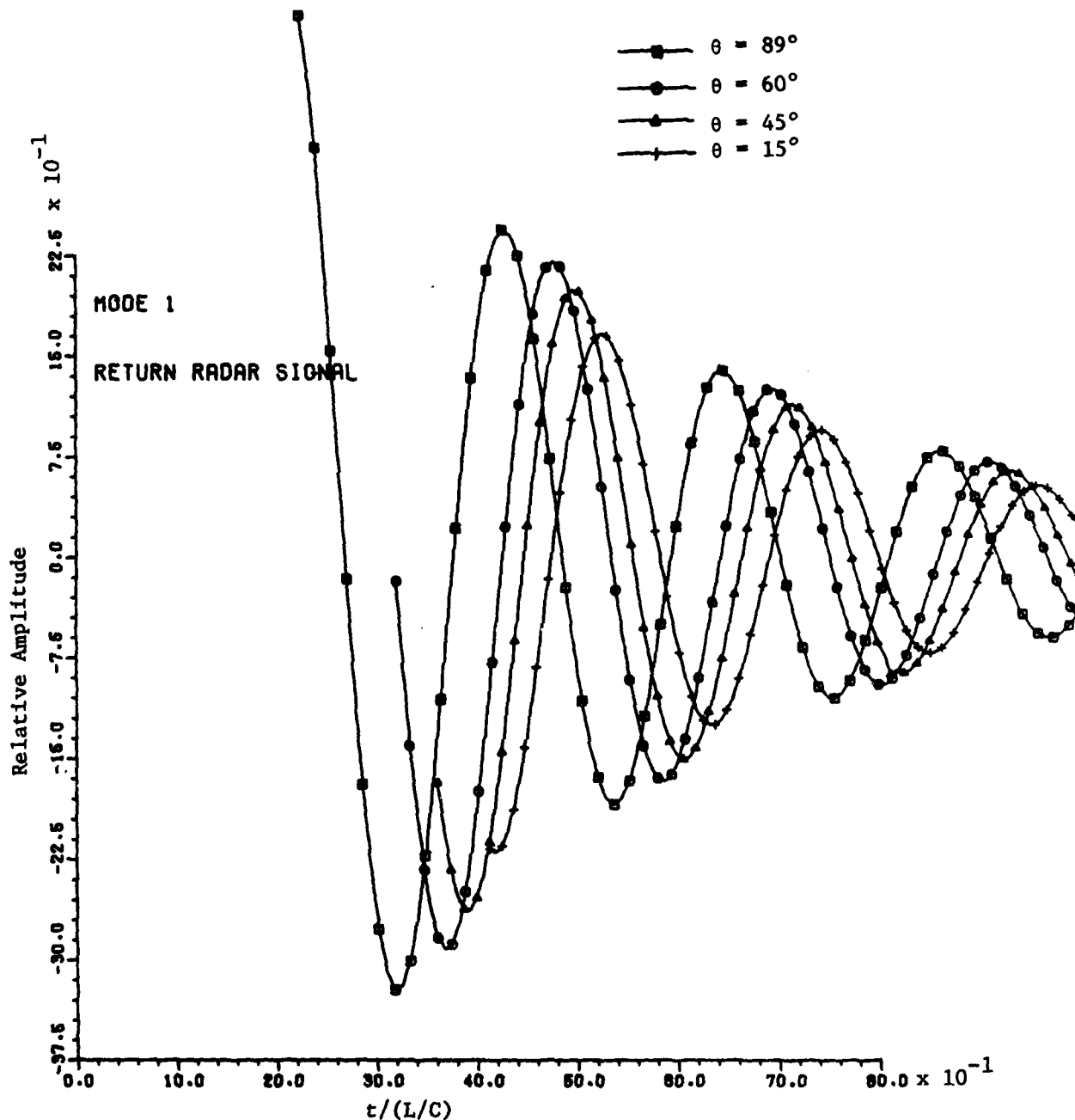


fig. 6. Return radar signals from a wire oriented at various angles, $\theta=15^\circ$, 45° , 60° and 89° , when it is illuminated by the incident radar signal which is synthesized for the first mode excitation.

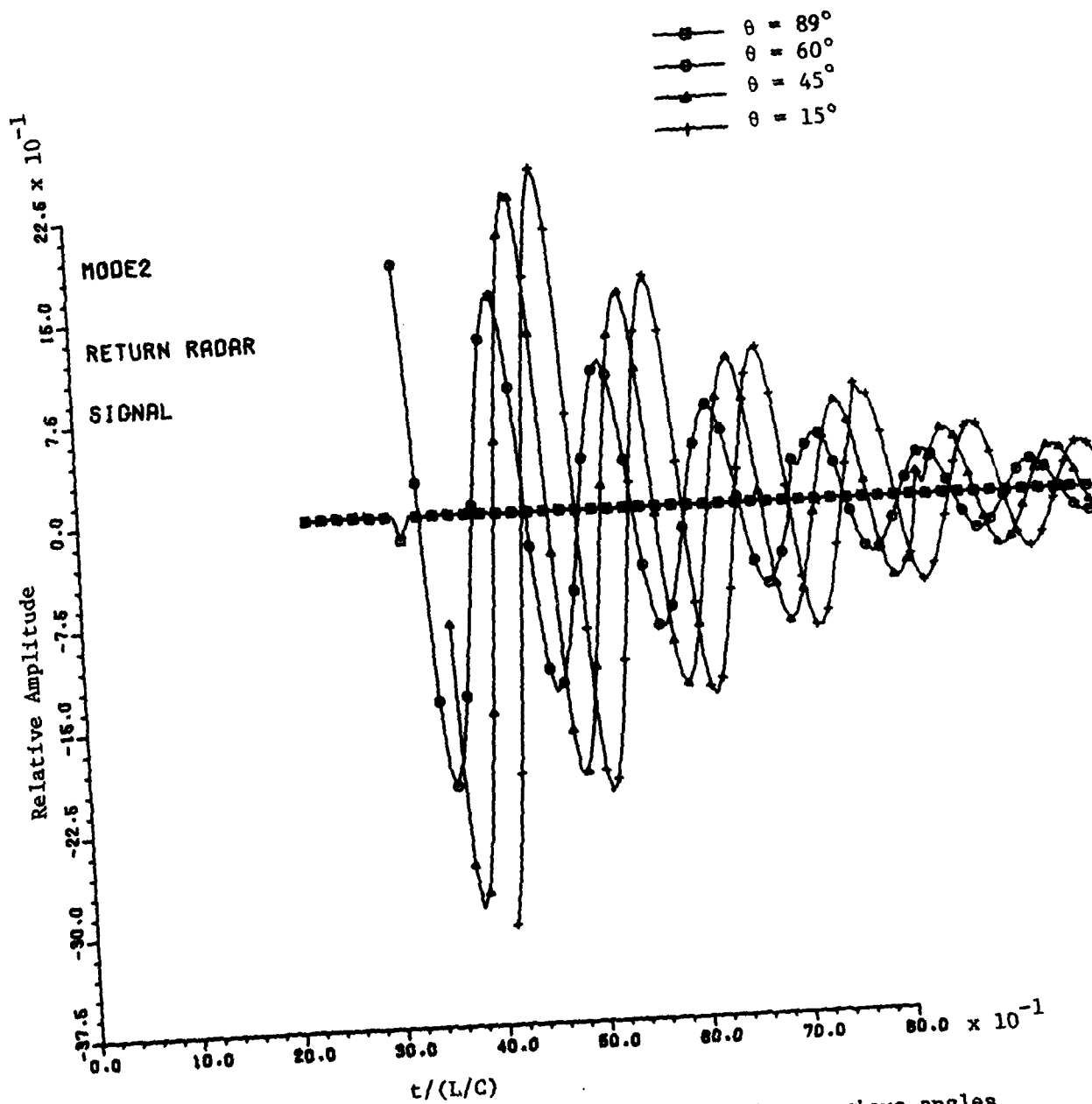


fig. 7. Return radar signals from a wire oriented at various angles of 15° , 45° , 60° and 89° , when it is illuminated by the incident radar signal which is synthesized for the second mode excitation.

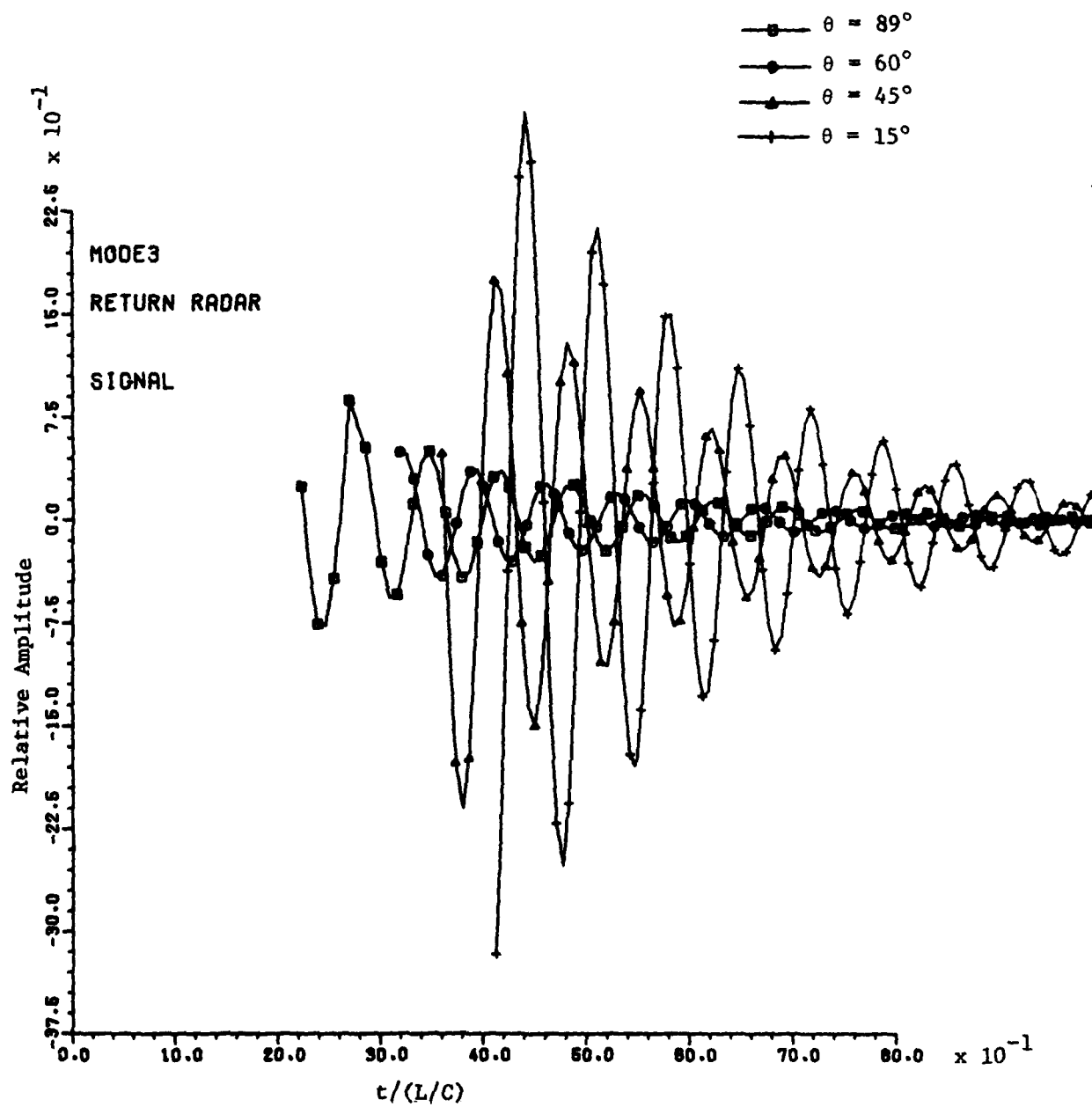


fig. 8. Return radar signals from a wire oriented at various angles of 15° , 45° , 60° and 89° , when it is illuminated by the incident radar signal which is synthesized for the third mode excitation.

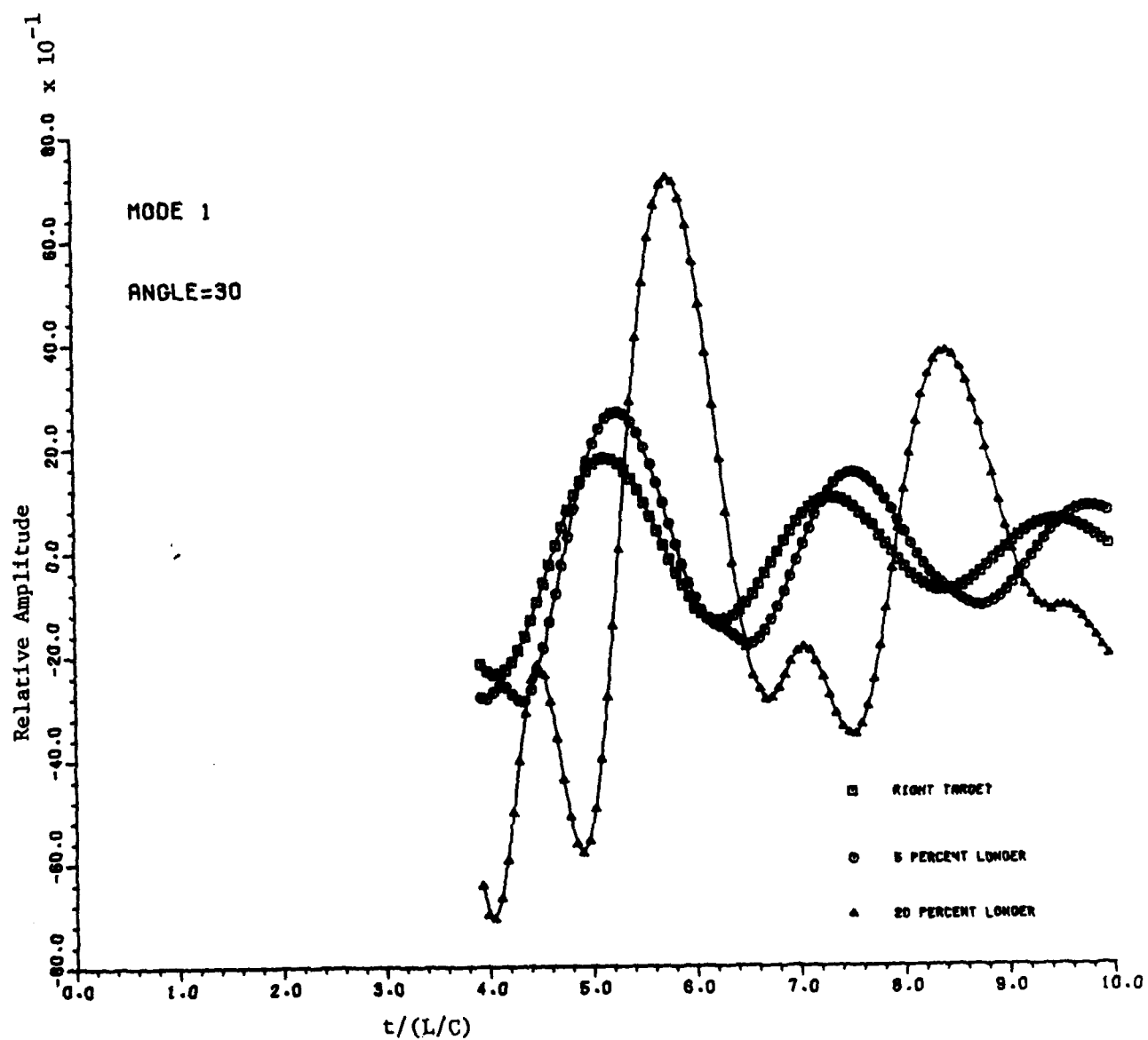


fig. 9. Return radar signals from three targets, the right target (wire), a wire 5% longer than the right target and a wire 20% longer, when they are illuminated at 30° aspect angle by the incident radar signal which is synthesized for exciting the first natural mode of the right target.

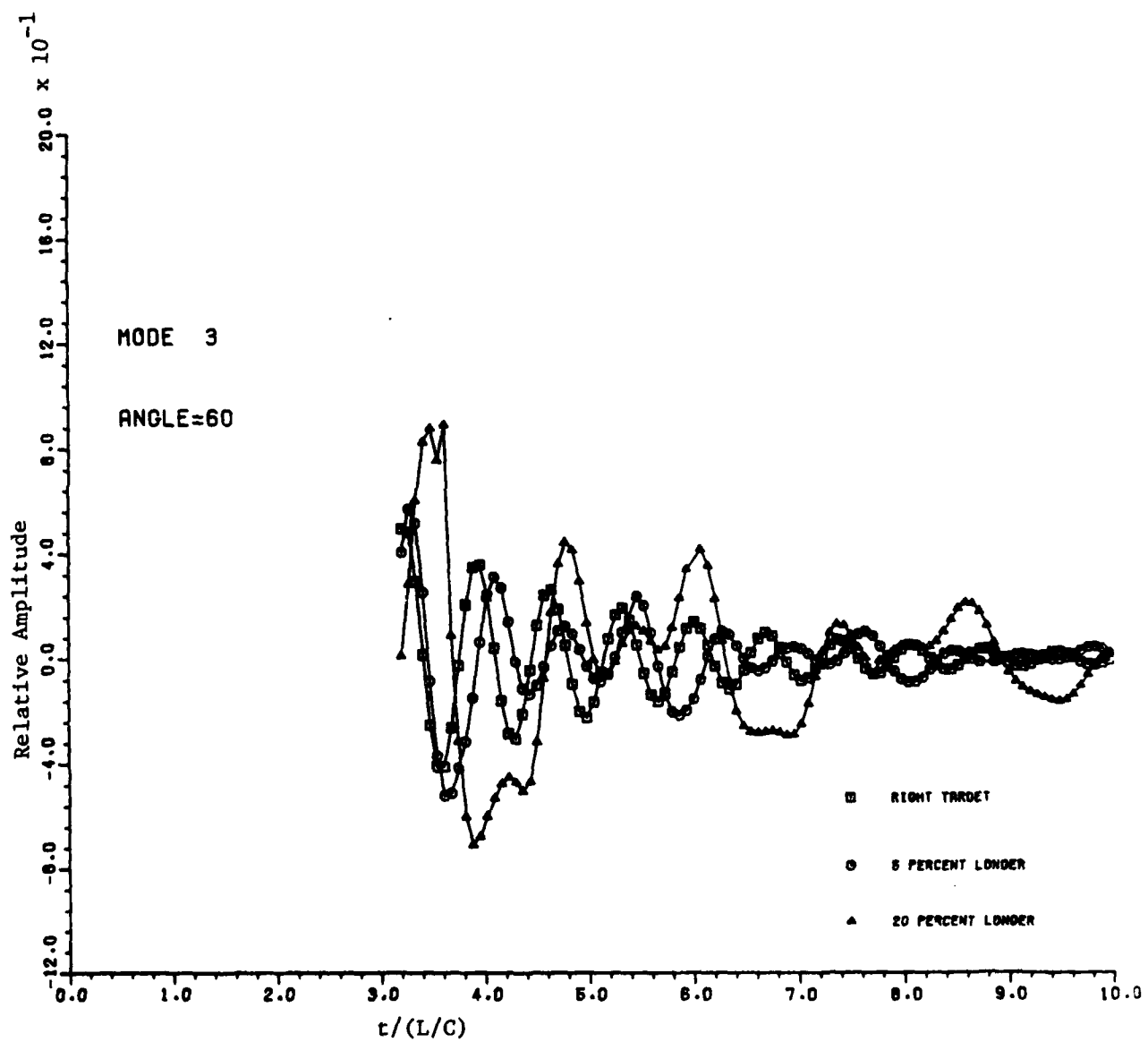


fig. 10. Return radar signals from three targets, the right target (wire), a wire 5% longer than the right target and a wire 20% longer, when they are illuminated at 60° aspect angle by the incident radar signal which is synthesized for exciting the third natural mode of the right target.

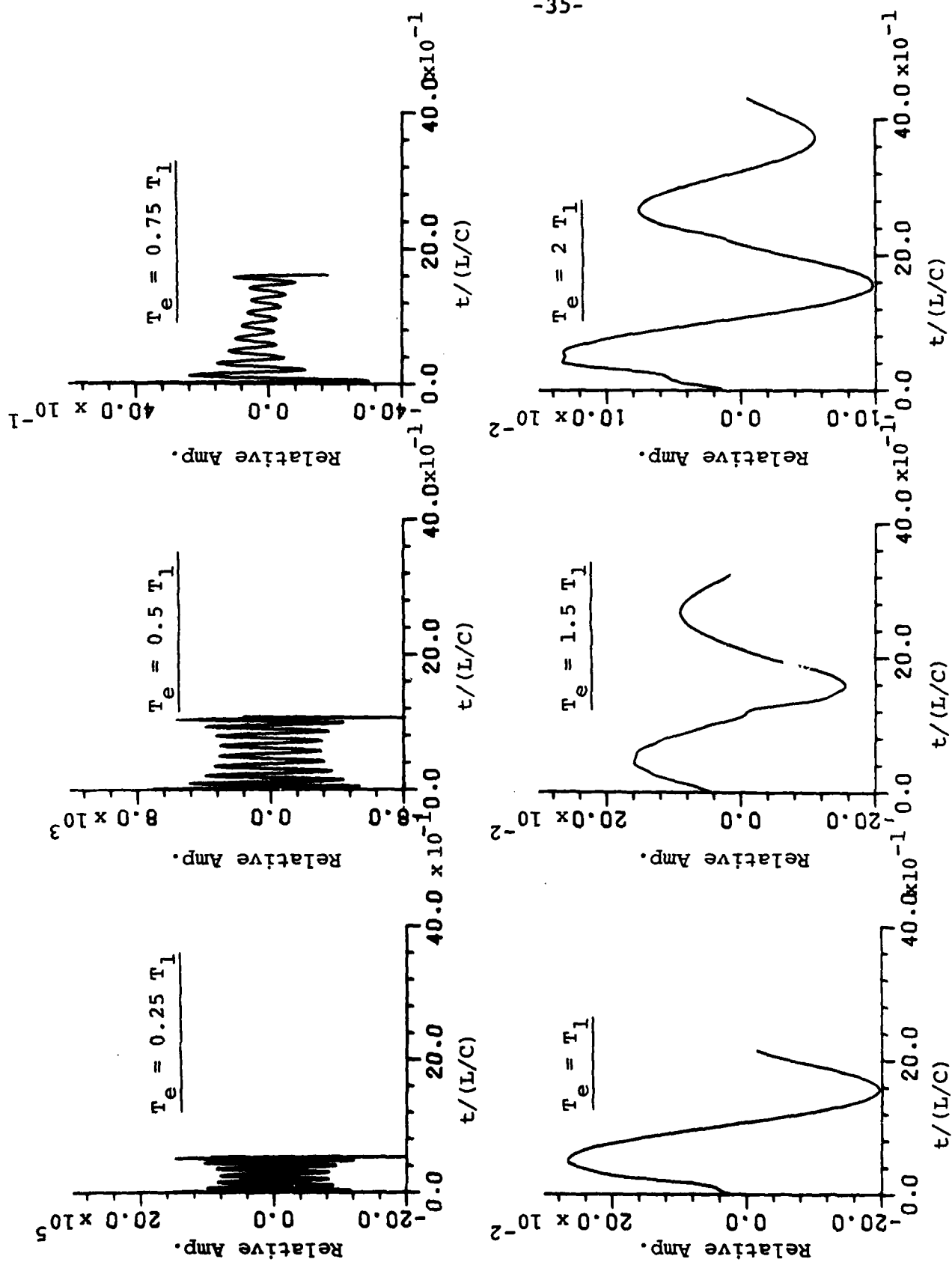


fig. 11. Required waveforms for the incident radar signal with various pulse durations to excite an arbitrarily oriented wire to produce a return signal which contains only the first natural mode of the wire. These required incident signals are aspect-independent.

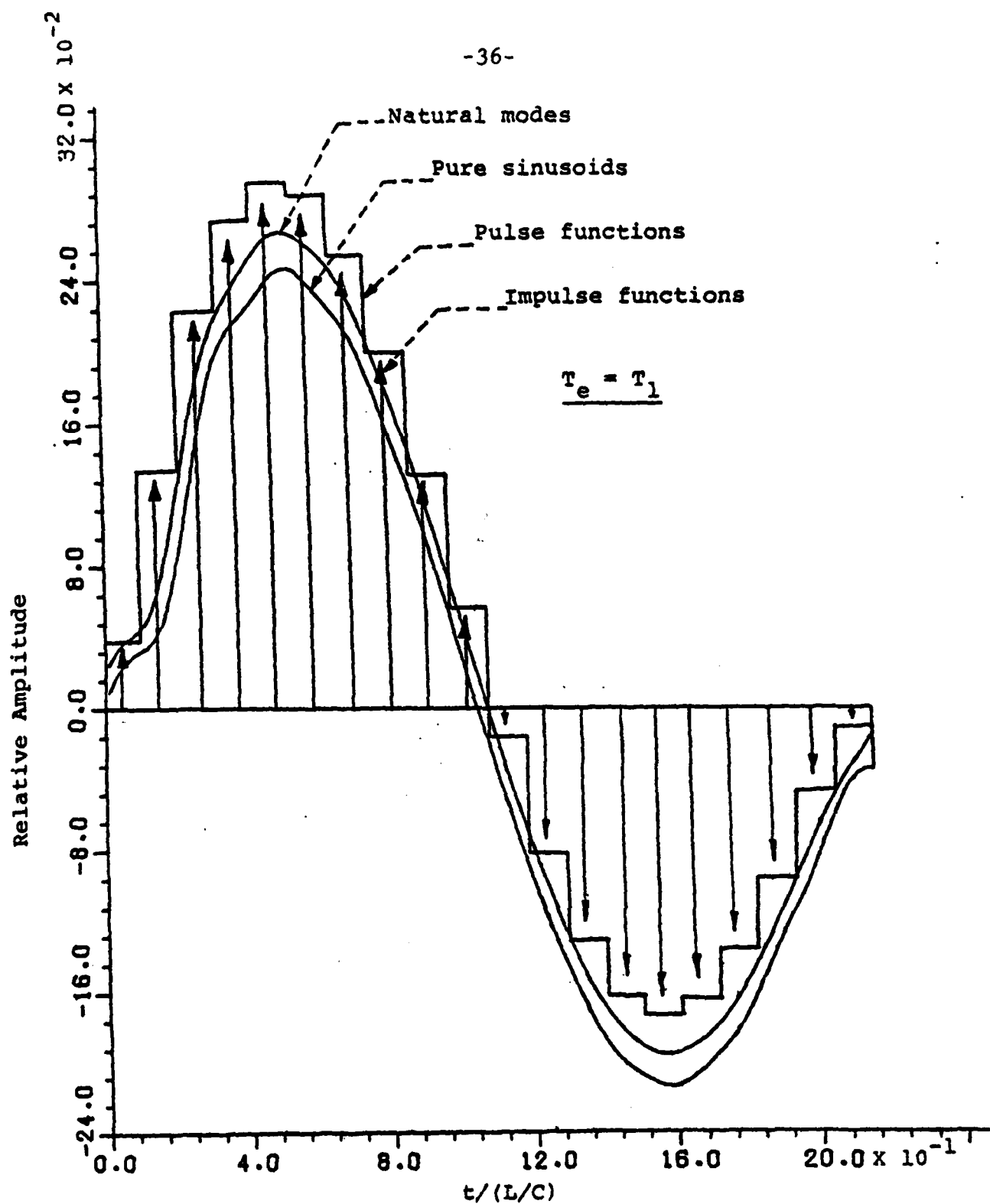


fig. 12. Required incident radar signals for exciting the first natural mode backscatter from an arbitrarily oriented wire of length L . These signals are constructed with natural modes of the wire, pure sinusoids with natural frequencies of the wire, pulse functions or impulse functions. The pulse duration of the signal is equal to a period of the first natural mode of the wire.

PART 2

RADAR WAVEFORM SYNTHESIS FOR EXCITING SINGLE-
MODE BACKSCATTERS FROM A SPHERE

1. Introduction

Techniques of using a short radar pulse to identify the radar target have been studied by a number of workers [1-6]. Typical scheme consists of illuminating the target with a radar pulse and then identify the target by identifying it with its natural modes that are extracted from the return signal. One of the problems associated with this scheme is difficulty in obtaining accurate natural frequencies of the target from a noisy return signal. In a recent study by our group, an inverse scheme, called the radar waveform synthesis method, has been investigated [7]. Instead of analyzing the return signal from the target in terms of its natural mode, this new scheme synthesizes the waveform of the incident radar signal in such a way that, when it excites the target, the return radar signal contains only a single natural mode of the target. It can be shown that when the incident radar signal synthesized to excite a particular natural mode of a preselected target is applied to a different target, the return signal will be significantly different from that of the expected natural mode. The wrong target can thus be sensitively discriminated.

In this paper, the geometry of a perfectly conducting sphere is used as the radar target. We aim to synthesize suitable incident radar signals which can be used to excite various single-mode backscatters from the sphere. To solve the problem, the scattered field from the sphere excited by an incident signal with an arbitrary waveform is determined in the spectral domain. The back-scattered field is then determined. An approximate impulse response in the time domain is obtained by summing up an infinite number of natural modes based on the Singularity Expansion Method. That impulse response is further approximated by the sum of finite numbers of damped sinusoids yielding an accurate result in the late-time period.

It is then demonstrated that a proper incident signal can be synthesized in such a way that when it excites the sphere, or when it convolutes with the impulse response, the return signal contains only a single natural mode of the sphere in the late-time period.

A method of synthesizing required incident signals for exciting various single-mode backscatters is presented. Numerical examples are given to show the required incident signals for various single-mode excitations and the resulting return signals which exhibit single natural mode of the sphere.

When an incident signal synthesized to excite a particular natural mode of a sphere is applied to a wrong sphere with a slightly different radius from that of the right sphere, the return signal from the wrong sphere is found to be significantly different from that of a natural mode of a sphere. The wrong sphere is, thus, sensitively discriminated from the right sphere. This indicates the applicability of the radar waveform synthesis method for radar target discrimination.

2. Theory

The geometry of the problem is shown in fig. 1 where a radar signal propagating in the $+z$ -direction is incident upon a perfectly conducting sphere which has radius a and has its center located at the origin of the coordinates. The electric field of the incident radar signal is assumed to be

$$\vec{E}^i(\vec{r}, t) = \hat{x} F(t - \frac{z+a}{c}) u(t - \frac{z+a}{c}) \quad (1)$$

where $F(t)$ is an unknown waveform function to be synthesized in such a way that $E^i(\vec{r}, t)$ excites a single-mode backscatter from the sphere. The Laplace transform of eq. (1) can be expressed as

$$\vec{E}^i(\vec{r}, s) = F(s) e^{-\gamma a} \hat{x} e^{-\gamma R} \cos\theta \quad (2)$$

where $\gamma = s/c$. When the unit vector \hat{x} is written in terms of spherical vector components, eq. (2) becomes

$$\vec{E}^i(\vec{r}, s) = F(s) e^{-\gamma a} [\sin\theta \cos\phi \hat{R} + \cos\theta \cos\phi \hat{\theta} - \sin\phi \hat{\phi}] e^{-\gamma R} \cos\theta \quad (3)$$

Since $\vec{E}^i(\vec{r}, s)$ satisfies the wave equation,

$$\nabla \times \nabla \times \vec{E} + \gamma^2 \vec{E} = 0, \quad (4)$$

$\vec{E}^i(\vec{r}, s)$ can be expressed in terms of spherical vector wave functions (see Appendix) as follows:

$$\vec{E}^i(\vec{r}, s) = F(s) e^{-\gamma a} \sum_{n=1}^{\infty} (a_n \vec{M}_{oln}^{(i)} + b_n \vec{N}_{eln}^{(i)}) \quad (5)$$

where

$$\vec{M}_{oln}^{(i)} = \frac{1}{\sin\theta} i_n(\gamma R) P_n^1(\cos\theta) \cos\phi \hat{R} - i_n(\gamma R) \frac{\partial P_n^1(\cos\theta)}{\partial \theta} \sin\phi \hat{\theta} \quad (6)$$

$$\begin{aligned} \vec{N}_{eln}^{(i)} = & \frac{n(n+1)}{\gamma R} i_n(\gamma R) P_n^1(\cos\theta) \cos\phi \hat{R} \\ & + \frac{1}{\gamma R} \frac{\partial}{\partial R} [R i_n(\gamma R)] \frac{\partial P_n^1(\cos\theta)}{\partial \theta} \cos\phi \hat{\theta} \\ & - \frac{1}{\gamma R \sin\theta} \frac{\partial}{\partial R} [R i_n(\gamma R)] P_n^1(\cos\theta) \sin\phi \hat{\phi} \end{aligned} \quad (7)$$

The superscript (i) for \vec{M} and \vec{N} functions stands for the use of $i_n(\gamma R)$ which is the first kind of the modified spherical Bessel function of order n. $P_n^1(\cos\theta)$ is the associated Legendre function of order n and degree 1. These functions are detailed in Appendix.

The coefficients a_n and b_n in eq. (5) can be determined by comparing eqs. (5) and (3) after $e^{-\gamma R \cos\theta}$ in eq. (3) is expanded into spherical harmonics [8] :

$$a_n = (-1)^n \frac{2n+1}{n(n+1)}, \quad b_n = (-1)^{n+1} \frac{2n+1}{n(n+1)} \quad (8)$$

Therefore, the incident electric field $\vec{E}^i(\vec{r}, s)$ can be expressed as

$$\vec{E}^i(\vec{r}, s) = F(s) e^{-\gamma a} \sum_{n=1}^{\infty} (-1)^n \frac{2n+1}{n(n+1)} \left[\vec{M}_{oln}^{(i)} - \vec{N}_{eln}^{(i)} \right] \quad (9)$$

Similarly, the scattered electric field from the sphere $\vec{E}^s(\vec{r}, s)$ can be expressed in terms of spherical vector functions as

$$\vec{E}^s(\vec{r}, s) = F(s) e^{-\gamma a} \sum_{n=1}^{\infty} (-1)^n \frac{2n+1}{n(n+1)} \left[c_n \vec{M}_{01n}^{(k)} - d_n \vec{N}_{e1n}^{(k)} \right] \quad (10)$$

where $\vec{M}_{01n}^{(k)}$ and $\vec{N}_{e1n}^{(k)}$ have the same expressions of $\vec{M}_{01n}^{(i)}$ and $\vec{N}_{e1n}^{(i)}$ as given in eqs. (6) and (7) except with their $i_n(\gamma R)$ function replaced by $k_n(\gamma R)$ function which is the second kind of modified spherical Bessel function. $k_n(\gamma R)$ function is needed to give attenuating behavior of the scattered field as R approaches to infinity.

The coefficient c_n and d_n in eq. (10) can be determined based on the boundary conditions on the spherical surface

$$E_\theta^i + E_\theta^s = 0 \quad \text{and} \quad E_\phi^i + E_\phi^s = 0 \quad \text{on } R = a,$$

to be

$$c_n = - \frac{i_n(\gamma a)}{k_n(\gamma a)} \quad (11)$$

$$d_n = - \frac{\frac{\partial}{\partial R} \left[R \frac{i_n(\gamma R)}{k_n(\gamma R)} \right]_{R=a}}{\frac{\partial}{\partial R} \left[R \frac{i_n(\gamma R)}{k_n(\gamma R)} \right]_{R=a}} \quad (12)$$

The final expression for the scattered electric field is

$$\vec{E}^s(\vec{r}, s) = - F(s) e^{-\gamma a} \sum_{n=1}^{\infty} (-1)^n \frac{2n+1}{n(n+1)} \left\{ \left[\frac{i_n(\gamma a)}{k_n(\gamma a)} \right] \vec{M}_{01n}^{(k)} - \left[\frac{\frac{\partial}{\partial R} (R \frac{i_n(\gamma R)}{k_n(\gamma R)})}{\frac{\partial}{\partial R} (R \frac{i_n(\gamma R)}{k_n(\gamma R)})} \right]_{R=a} \vec{N}_{e1n}^{(k)} \right\} \quad (13)$$

The backscattered electric field in the far zone of the sphere should be in the x -direction, parallel to the direction of the incident electric field, and can be found from

$$\vec{E}^s = \hat{x} \left[E_\theta^s \right]_{R=\infty, \theta=\pi, \phi=\pi} \quad (14)$$

Since as R approaches to infinity,

$$k_n(\gamma R) \rightarrow \frac{\pi}{2} \frac{1}{\sqrt{R_\infty}} e^{-\gamma R_\infty} \text{ and } \frac{1}{\sqrt{R}} \frac{\partial}{\partial R} (R k_n(\gamma R)) \rightarrow -\frac{\pi}{2} \frac{1}{\sqrt{R_\infty}} e^{-\gamma R_\infty}$$

and

$$\left[\frac{P_n^1(\cos\theta)}{\sin\theta} \right]_{\theta=\pi} = -\frac{(-1)^n}{2} n(n+1), \quad \left[\frac{\partial P_n^1(\cos\theta)}{\partial\theta} \right]_{\theta=\pi} = \frac{(-1)^n}{2} n(n+1),$$

as $R \rightarrow \infty$, $\theta=\pi$ and $\phi=\pi$, $\vec{M}_{01n}^{(k)}$ and $\vec{N}_{e1n}^{(k)}$ functions become

$$\vec{M}_{01n}^{(k)} = \vec{N}_{e1n}^{(k)} \rightarrow \hat{\theta} \frac{\pi}{2} \frac{1}{\sqrt{R_\infty}} e^{-\gamma R_\infty} \frac{(-1)^n}{2} n(n+1).$$

Thus, the backscattered electric field becomes

$$\vec{E}^s(s) = -\hat{x} \frac{\pi}{4} F(s) \frac{e^{-\gamma(R_\infty+a)}}{\sqrt{R_\infty}} \sum_{n=1}^{\infty} (2n+1) \left\{ \frac{i_n(\gamma a) \frac{\partial}{\partial R} [R k_n(\gamma R)]_{R=a} - \frac{\partial}{\partial R} [R i_n(\gamma R)]_{R=a} k_n(\gamma a)}{k_n(\gamma a) \frac{\partial}{\partial R} [R k_n(\gamma R)]_{R=a}} \right\} \quad (15)$$

Using the following Wronskian,

$$i_n(x) \frac{\partial}{\partial x} [x k_n(x)] - k_n(x) \frac{\partial}{\partial x} [x i_n(x)] = -\frac{\pi}{2} \left(\frac{1}{x} \right) \quad (16)$$

eq. (15) can be simplified to be

$$\vec{E}^s(s) = \hat{x} \frac{\pi^2}{8} F(s) \frac{e^{-\gamma(R_\infty+a)}}{R_\infty a} \frac{1}{\gamma^2} \sum_{n=1}^{\infty} \frac{2n+1}{k_n(\gamma a) \left[\frac{\partial}{\partial R} (R k_n(\gamma R)) \right]_{R=a}} \quad (17)$$

The backscattered electric field \vec{E}^s given in eq. (17) can be developed further because the modified spherical Bessel functions can be expressed with truncated power serieses as follows [9].

$$k_n(\zeta) = \frac{\pi}{2} \frac{e^{-\zeta}}{\zeta} \sum_{\beta=0}^n \frac{(n+\beta)!}{\beta!(n-\beta)!} (2\zeta)^{-\beta} \quad (18)$$

$$\frac{\partial}{\partial \zeta} \left[\zeta k_n(\zeta) \right] = -\frac{\pi}{2} e^{-\zeta} \sum_{n=0}^{\infty} \frac{(n+\beta)!}{\beta!(n-\beta)!} (1+\frac{\beta}{\zeta}) (2\zeta)^{-\beta} \quad (19)$$

If eqs. (18) and (19) are substituted in eq. (17), we have the final expression for $\vec{E}^s(s)$ as

$$\vec{E}^s(s) = -\hat{x} \frac{1}{2} \frac{a}{R_\infty} e^{-\gamma(R_\infty - a)} F(s) \sum_{n=1}^{\infty} \frac{(2n+1)\zeta^{2n}}{f_n(\zeta)g_n(\zeta)} \quad (20)$$

where

$$f_n(\zeta) = \sum_{\beta=0}^n \frac{(n+\beta)!}{\beta!(n-\beta)!} \frac{1}{2^\beta} \zeta^{n-\beta} \quad (21)$$

$$g_n(\zeta) = \sum_{\beta=0}^n \frac{(n+\beta)!}{\beta!(n-\beta)!} \frac{1}{2^\beta} (\beta+\zeta) \zeta^{n-\beta} \quad (22)$$

$$\zeta = \gamma a \quad \text{and} \quad \gamma = s/c.$$

R_∞ = distance between the observation point and the center of the sphere.

The backscattered electric field can also be expressed as

$$\vec{E}^s(s) = -\hat{x} \frac{a}{2R_\infty} e^{-s(R_\infty - a)/c} F(s) H(s) \quad (23)$$

where

$$H(s) = \sum_{n=1}^{\infty} \frac{(2n+1)\zeta^{2n}}{f_n(\zeta)g_n(\zeta)} \quad \text{with} \quad \zeta = \frac{a}{c} s \quad (24)$$

In eq. (23), $F(s)$ is the unknown function describing the waveform of the incident radar signal, and $H(s)$ is the transfer function of

the sphere. The transfer function $H(s)$ as expressed in eq. (24) is a poorly converging infinite series and its evaluation for large value of ζ requires sophisticated Watson's transformation [10] or extensive Fourier-numerical method [11]. To synthesize an incident radar signal which excites a single-mode backscatter from a sphere, it is necessary to obtain a reasonably accurate impulse response which is the Laplace inverse transform of $H(s)$. This is done in the next section.

3. Impulse Response

The impulse response $h(\tau)$ is obtained by inverting $H(s)$. In the process of inverting $H(s)$, the roots of $f_n(\zeta)$ and $g_n(\zeta)$ functions in eq. (24) are computed based on Müller's algorithm. There are n roots for each $f_n(\zeta)$ function and $n+1$ roots for each $g_n(\zeta)$ function, as can be seen easily from eqs. (21) and (22). If these roots are plotted in the s -plane (or the ζ -plane), they can be grouped into branches of roots as shown in fig. 2. Except those roots lying on the negative real axis, all other roots are in conjugate pairs. These roots indicate the locations of the simple poles of $H(s)$ in the s -plane. It is noted that the roots in one branch come from either $f_n(\zeta)$ or $g_n(\zeta)$ but they do not belong to the same index n . For example, the first branch (and other odd-numbered branches) of roots come from $g_n(\zeta)$ functions of various n , and the second branch (and other even-numbered branches) of roots come from $f_n(\zeta)$ function of various n . Through numerical calculation, we found that this kind of regrouping the roots in the s -plane provides an interesting information; asymptotically, the roots belonging to the same branch have a simple arithmetic relation between their locations on the s -plane, and the residues of $H(s)$ at these roots (or poles) possess a simple geometric relation between their complex amplitudes.

For simplicity, we can designate the roots with the symbol, ζ_{ij} , where the subscript i represents the i th branch and the subscript j means the j th root of the branch. Also we can use $j=0$ to designate those roots lying on the negative real axis. In general, we can express

$$\zeta_{ij} = \sigma_{ij} + j\omega_{ij}, \zeta_{ij}^* = \sigma_{ij} - j\omega_{ij} \text{ and } \zeta_{i0} = \sigma_{i0},$$

The transfer function $H(s)$ contains only simple poles located at these roots and the residues of $H(s)$ evaluated at these poles are given by

$$[\text{Res } H(s)]_{\text{at } \zeta_{ij}} = a_{ij} = a_{ij}^r + j a_{ij}^i, [\text{Res } H(s)]_{\text{at } \zeta_{ij}^*} = a_{ij}^* = a_{ij}^r - j a_{ij}^i.$$

Some lower-order roots and the corresponding residues of $H(s)$ are tabulated in Table 1.

The transfer function $H(s)$ can be expanded into an infinite series as

$$H(s) = \sum_{i=1}^N \sum_{j=1}^{\infty} \left(\frac{a_{ij}}{\zeta - \zeta_{ij}} + \frac{a_{ij}^*}{\zeta - \zeta_{ij}^*} \right) + \sum_{i=2}^N \frac{a_{i0}}{\zeta - \zeta_{i0}} \quad (25)$$

The summation of the second term of eq. (25) starts from $i=2$ because there is no root of the first branch lying on the negative real axis. The upper limit of the summation over i , N , is dictated by the maximum number of the branches needed to be considered. Numerically it was found that a reasonably accurate solution can be obtained with N less than 3.

The impulse response can then be obtained as

$$h(\tau) = \left(\frac{c}{a} \right) \sum_{i=1}^N \sum_{j=1}^{\infty} 2 \text{Re}(a_{ij} e^{\zeta_{ij} \tau}) + \left(\frac{c}{a} \right) \sum_{i=2}^N a_{i0} e^{\zeta_{i0} \tau} \quad (26)$$

where $\tau = t/(a/c)$ is a normalized time, and each term of eq. (26) represents a natural mode of the sphere.

Examining Table 1, one can observe a simple arithmetic relation between the values of roots (or the locations of poles) belonging to the same branch if j is bigger than 10. That is,

$$\zeta_{ij} - \zeta_{ij-1} = \Delta\zeta_i \rightarrow \text{constant, if } j > 10. \text{ For example,}$$

$$\Delta\zeta_1 = -0.035 + j0.98 \text{ and } \Delta\zeta_2 = -0.078 + j0.96 \text{ for } j > 19.$$

Similarly, there is a simple geometric relation between the residues at these poles of the same branch if j is bigger than 10. That is, $a_{ij}/a_{ij-1} = R_i \rightarrow \text{constant}$, if $j > 10$. For example, $R_1 = 1.09 e^{j1.18}$ and $R_2 = 1.19 e^{j1.22}$ for $j > 19$.

In view of these simple relations, the infinite sum of the modes in eq. (26) can be divided into two parts; the first part is the sum of the first 10 or 20 terms and the second part is the sum of the rest of the terms. For example, we can sum the modes coming from the poles of the first branch, $i=1$, as

$$[h(\tau)]_1 = \left(\frac{c}{a}\right)_2 \operatorname{Re} \sum_{j=1}^{19} a_{1j} e^{\zeta_{1j}\tau} + \left(\frac{c}{a}\right)_2 \operatorname{Re} \sum_{j=20}^{\infty} a_{1j} e^{\zeta_{1j}\tau} \quad (27)$$

Now the simple relations between roots and residues for large j can be used to approximate the last term of eq. (27) as an infinite geometric series which is then summed up to be

$$\begin{aligned} 2 \operatorname{Re} \sum_{j=20}^{\infty} a_{1j} e^{\zeta_{1j}\tau} &= 2 \operatorname{Re} \left\{ a_{1,19} e^{\zeta_{1,19}\tau} \left[R_1 e^{\Delta\zeta_1\tau} + (R_1 e^{\Delta\zeta_1\tau})^2 + \dots + (R_1 e^{\Delta\zeta_1\tau})^{\infty} \right] \right\} \\ &= 2 \operatorname{Re} \left[a_{1,19} e^{\zeta_{1,19}\tau} \left(\frac{R_1 e^{\Delta\zeta_1\tau}}{1 - R_1 e^{\Delta\zeta_1\tau}} \right) \right] \end{aligned} \quad (28)$$

The fact that $\Delta\zeta_1$ contains a negative real part has been used, and eq. (28) is valid for $\tau > 0$. For $\tau = 0$, the impulse response can be shown to be infinite, directly from eq. (24) based on the initial value theorem.

If numerical values of $a_{1,19}$, $\zeta_{1,19}$, R_1 and $\Delta\zeta_1$ are substituted in eq. (28), we have

$$\begin{aligned} 2 \operatorname{Re} \left[\sum_{j=20}^{\infty} a_{1j} e^{\zeta_{1j}\tau} \right] &= \\ \frac{89.34 e^{-1.797\tau} [\cos(19.32\tau - 0.485) - 1.09 e^{-0.035\tau} \cos(18.34\tau - 1.66)]}{1 + 1.19 e^{-0.07\tau} - 2.18 e^{-0.035\tau} \cos(0.98\tau + 1.18)} \end{aligned} \quad (29)$$

The first term of eq. (27) can be easily summed up numerically, and when it is combined with eq. (29) the part of the impulse response, $h(\tau)$, which is contributed by the modes of the first branch poles, can be computed as a function of time. It was found that a reasonably good result can be obtained just considering the contribution from the poles of the first branch.

A numerical example is given in Figs. 3 and 4. Fig. 3 shows the impulse response computed from the sum of the first 19 pairs of the poles of the first branch, or the first term of eq. (27). It shows a strong oscillatory response in the early-time period, but no creeping wave peak is observed. This result is wrong, judging from the existing results. However, if the term given in eq. (29), which represents the contribution due to the rest of the poles of the first branch, is added to the contribution from the first 19 pairs of the poles, a surprising result is obtained; the strong oscillatory response during the early-time period is cancelled and a sharp peak representing the creeping wave contribution appears at $\tau = t(c/a) = 5.25$, as shown in Fig. 4. It is noted that an impulse at $t=0$ is added in Fig. 4, as it should be. The impulse response shown in Fig. 4 agrees with the existing results. An approximate impulse response based on Fourier-numerical method [11] is included in Fig. 4 for comparison. If the contribution from the poles of other branches is considered, the accuracy of the impulse response during the early-time period can be improved. It is noted that if more than 19 pairs of poles in the first branch are considered without the compensation of a corresponding correction term, the oscillatory response in the early-time period becomes stronger instead of weaker. This is due to the fact that the amplitude (residue) of the mode increases with the order of the mode (Table 1). For many practical applications the result of Fig. 4 is sufficient.

For our purpose of synthesizing an incident radar signal which excites a single-mode backscatter from a sphere, it is desirable to obtain an approximate impulse response in the form of a truncated sum of natural modes. To do so, it is necessary to approximate the

correction term of eq. (29) with two damped sinusoids which possess the forms of natural modes. This step was accomplished numerically by the cut and try approach. We found the two damped sinusoids, $1.34 e^{-2.0\tau} \cos(18.891\tau + .4838)$ and $.127 e^{-.55\tau} \cos(19.50\tau - .7159)$, can approximate the correction term of eq. (29) quite well for $\tau > 2$. Since we aim to synthesize a required incident radar signal for exciting a single-mode backscatter in the late-time period, we do not need the information on the early-time behavior of the impulse response. The approximate impulse response constructed with the first 19 natural modes of the first branch and two damped sinusoids which approximate the correction term of eq. (29) is shown in Fig. 5. This approximate impulse response approximates the true impulse response quite accurately for $\tau > 2$. Thus, it will be used in the synthesis of the incident radar signal for exciting a single-mode backscatter in the late-time period.

4. Excitation of Simple-Mode Backscatter

The approximate impulse response of a sphere can be represented by the first 19 natural modes from the first branch of poles, two damped sinusoids which approximate the correction term of eq. (29) for $\tau \geq 2$, and a term which compensates the error for the early-time period of $0 \leq \tau \leq 2$. Symbolically, we can express the impulse response $h(\tau)$ as

$$h(\tau) = \sum_{n=1}^{21} a_n e^{\sigma_n \tau} \cos(\omega_n \tau + \phi_n) + \xi(\tau) \quad (30)$$

In eq. (30), the first 19 terms of the summation,

$\sum_{n=1}^{19} a_n e^{\sigma_n \tau} \cos(\omega_n \tau + \phi_n)$, represent the sum of the first 19 natural modes from the first branch of poles. The last two terms of the summation, $\sum_{n=20}^{21} a_n e^{\sigma_n \tau} \cos(\omega_n \tau + \phi_n)$, represent the two damped sinusoids which approximate the correction term of eq. (29) for $\tau \geq 2$, i.e.,

$$a_{20} e^{\sigma_{20}\tau} \cos(\omega_{20}\tau + \phi_{20}) = \left(\frac{c}{a}\right) 1.34 e^{-2.01\tau} \cos(18.891\tau + .4858)$$

$$a_{21} e^{\sigma_{21}\tau} \cos(\omega_{21}\tau + \phi_{21}) = \left(\frac{c}{a}\right) 0.127 e^{-5.55\tau} \cos(19.50\tau - .7159).$$

The term $\xi(\tau)$ exists only during the period of $0 \leq \tau \leq 2$, and is the term to be added to the summation term of eq. (31) to yield an accurate impulse response for that period of time because with only the summation term of eq. (31) it does not give accurate result for $h(\tau)$ during that early-time period. The function $\xi(\tau)$ is difficult to determine but it is not needed if we only aim to produce a single-mode backscatter in the late-time period.

We now aim to synthesize an incident electric field $E^i(\tau)$ of duration τ_e in such a way that when it illuminates the sphere, the backscattered electric field $E^s(\tau)$ consists only of a single natural mode in the late-time period of $\tau \geq \tau_e + 2$. The backscattered electric field $E^s(\tau)$ can be expressed, based on the convolution theorem, as

$$\begin{aligned} E^s(\tau) &= \int_0^\tau e^{-E^i(\tau')} h(\tau - \tau') d\tau' \\ &= \int_0^\tau e^{-E^i(\tau')} \left[\sum_{n=1}^{21} a_n e^{\sigma_n(\tau-\tau')} \cos(\omega_n(\tau-\tau') + \phi_n) + \xi(\tau-\tau') \right] d\tau' \end{aligned} \quad (31)$$

If the normalized observation time $\tau \geq \tau_e + 2$, the term $\xi(\tau-\tau')$ does not contribute to the integral because $\xi(\tau) = 0$ for $\tau \geq 2$. Thus, eq. (31) becomes

$$\begin{aligned} E^s(\tau) &= \int_0^{\tau_e} E^i(\tau') \left[\sum_{n=1}^{21} a_n e^{\sigma_n(\tau-\tau')} \cos(\omega_n(\tau-\tau') + \phi_n) \right] d\tau' \\ &= \sum_{n=1}^{21} a_n e^{\sigma_n \tau} \left[A_n \cos(\omega_n \tau + \phi_n) + B_n \sin(\omega_n \tau + \phi_n) \right] \quad (32) \end{aligned}$$

for $\tau \geq \tau_e + 2$.

where the coefficients A_n and B_n are defined as

$$\begin{Bmatrix} A_n \\ B_n \end{Bmatrix} = \int_0^{\tau_e} E^i(\tau') e^{-\sigma_n \tau'} \begin{Bmatrix} \cos \omega_n \tau' \\ \sin \omega_n \tau' \end{Bmatrix} d\tau' \quad (33)$$

Based on eq. (33), it is now possible to choose an optimal $E^i(\tau)$ in such a way that all the coefficients vanish except one; by so doing, $E^s(\tau)$ will consist of a single natural mode.

5. Required Incident Signals and Return Signals

It is possible to choose an $E^i(\tau)$ to excite a single-mode $E^s(\tau)$. Consider an incident electric field $E^i(\tau)$ constructed from a linear combination of 21 damped sinusoids, 19 natural modes and two damped sinusoids approximating the correction term of eq. (29), as that appeared in eq. (30):

$$E^i(\tau) = \sum_{m=1}^{21} e^{\sigma_m \tau} (b_m \cos \omega_m \tau + c_m \sin \omega_m \tau) \quad (34)$$

where $\zeta_m = \sigma_m + j\omega_m$ is the m 'th natural frequency and ζ_{20} and ζ_{21} are the equivalent values of the two damped sinusoids, and b_m and c_m are unknown coefficients to be determined based on the requirement that only a single-mode $E^s(\tau)$ be excited.

Substituting representation (34) in eq. (33) leads to

$$A_n = \sum_{m=1}^{21} M_{nm}^1 b_m + \sum_{m=1}^{21} M_{nm}^2 c_m \quad (35)$$

$$B_n = \sum_{m=1}^{21} M_{nm}^3 b_m + \sum_{m=1}^{21} M_{nm}^4 c_m \quad (36)$$

where

$$\begin{Bmatrix} M_{nm}^1 \\ M_{nm}^2 \\ M_{nm}^3 \\ M_{nm}^4 \end{Bmatrix} = \int_0^{\tau_e} e^{-(\sigma_n - \sigma_m)\tau'} \begin{Bmatrix} \cos \omega_n \tau' \cos \omega_m \tau' \\ \cos \omega_n \tau' \sin \omega_m \tau' \\ \sin \omega_n \tau' \cos \omega_m \tau' \\ \sin \omega_n \tau' \sin \omega_m \tau' \end{Bmatrix} d\tau' \quad (37)$$

It is observed that the M_{nm}^i 's are explicit functions of incident radar pulse duration τ_e , and τ_e is a parameter of freedom which can be varied to obtain a desirable $E^i(\tau)$ waveform.

The unknown coefficients b_m and c_m can be solved for from eqs. (35) and (36) as

$$\begin{Bmatrix} b_1 \\ b_2 \\ \vdots \\ b_{21} \\ \hline c_1 \\ c_2 \\ \vdots \\ c_{21} \end{Bmatrix} = \begin{Bmatrix} M_{nm}^1 & M_{nm}^2 \\ \vdots & \vdots \\ M_{nm}^3 & M_{nm}^4 \end{Bmatrix}^{-1} \begin{Bmatrix} A_1 \\ A_2 \\ \vdots \\ A_{21} \\ \hline B_1 \\ B_2 \\ \vdots \\ B_{21} \end{Bmatrix} \quad (38)$$

In eq. (38), matrix $[M_{nm}]$ is of 42×42 order, while $\begin{Bmatrix} b_i \\ c_i \end{Bmatrix}$ and $\begin{Bmatrix} A_i \\ B_i \end{Bmatrix}$ are two column 42 matrices.

To obtain a single-mode scattered field (e.g., the j 'th mode), it is required that $B_j = 1$ and $B_n = 0$ for $n \neq j$ and $A_n = 0$ for all n . b_m and c_m are easily determined from eq. (38), and $E^i(\tau)$ is subsequently obtained from representation (34). With this $E^i(\tau)$, the scattered field, $E^s(\tau)$, becomes single-mode and can be expressed as

$$E^s(\tau) = a_j e^{\sigma_j \tau} \sin(\omega_j \tau + \phi_j) \quad (39)$$

Some numerical results on the required incident signals for exciting various single-mode backscatters and resulting single-mode return signals are shown in Figs. 6 and 7. Figure 6 shows the required incident signal for exciting the first-mode backscatter ($\zeta_1 = -0.5 + j0.866$) and the return signal which indeed shows the first natural mode in the late-time period of $\tau > 9$. The duration of the required incident signal is set to be one period of the first natural mode,

$$\tau_e = \tau_1 = \frac{1}{f_1} = \frac{2\pi}{\omega_1} = \frac{2\pi}{0.866} = 7.26.$$

The waveform of the required incident signal is found to contain a rapidly oscillatory component in the initial stage. However, the return signal contains only the much slower varying, first natural mode in the late-time period. This phenomenon is different from the case of a thin wire where the required incident signal for single-mode excitation consists mainly of the wanted natural mode [7]. The reason is that the natural modes of a thin wire are nearly orthogonal while that of a sphere are not orthogonal due to their large damping coefficients. It is noted that the return signal was obtained by convoluting the required incident signal with the approximate impulse response given in eq. (30). The early-time part of the return signal exhibits an irregular waveform and is not shown in the figure for the sake of clarity.

Figure 7 shows the required incident signal for exciting the third-mode backscatter ($\zeta_3 = -0.843 + j2.758$) and the return signal which contains only the third natural mode in the late-time period of $\tau > 9$. The required incident signal has a duration of one period of the first natural mode, and its waveform consists of a rapidly oscillatory component superimposed on a slowly varying component. The third-mode return signal was created by the numerical convolution of the required incident signal with the approximate impulse response.

The required incident signals for exciting the first and the third-mode backscatter appear to be somewhat irregular in waveform.

However, they can be constructed with 21 natural modes of appropriate amplitudes and phase angles as shown in Table 2. It appears that higher amplitudes for higher-order natural modes are needed to construct the required incident signal.

The relation between the signal duration and the waveform of the required incident signal was also studied. It was found that when the signal duration is shortened, the waveform of the required incident signal resembles that shown in Fig. 6 or Fig. 7 but it contains a more rapidly oscillatory component in the initial stage.

5. Target Discrimination

To show the capability of target discrimination of this method, two numerical examples are given in Figs. 8 and 9. Figure 8 shows the return signals from two spheres, the right sphere and a wrong sphere which radius is 10% smaller than that of the right sphere, when they are illuminated by the required incident signal for exciting the first-mode backscatter from the right sphere as that shown in Fig. 6. It is observed that the return signal from the right sphere is a pure first natural mode while that from the wrong sphere shows distortions in its waveform. Figure 9 shows the return signals from the same two spheres when they are illuminated by the required incident signal for exciting the third-mode backscatter from the right sphere as that shown in Fig. 7. The return signal from the right sphere is a pure third natural mode while that from the wrong sphere exhibits an irregular waveform. From these two examples, it is evident that the wrong target can be sensitively discriminated from the right target if the incident signals are properly synthesized for single-mode excitation. It is noted that if the wrong target were a thin wire or some other non-spherical object, the return signals from the wrong target would be entirely different from the natural modes of a sphere, and the discrimination of the wrong target from the right target would be trivial in that case.

6. Conclusion

It has been demonstrated that by expressing the backscattered field of a sphere in terms of its natural modes, it is possible to

synthesize an incident radar signal of appropriate waveform in such a way that when it illuminates the sphere, the return signal contains only a single natural mode of the sphere in the late-time period. When that synthesized incident signal is applied to a wrong target, the waveform of the return signal will be significantly different from that of natural modes of the sphere; thus, the wrong target can be sensitively discriminated from the right target. Since a single-mode radar return contains a narrow frequency band it may lead to improved signal-to-noise ratio and can be processed by narrow-band filters and amplifiers.

Appendix: Solutions of Wave Equation in Terms of Spherical Vector Wave Functions.

Consider the wave equation for the Laplace transformed \vec{E} field:

$$\nabla \times \nabla \times \vec{E} + \gamma^2 \vec{E} = 0 \quad (A1)$$

where $\gamma = s/c$.

To solve eq. (A1), we consider first the corresponding scalar wave equation,

$$\nabla^2 g - \gamma^2 g = 0 \quad (A2)$$

Assuming $g(R, \theta, \phi) = g_1(R)g_2(\theta)g_3(\phi)$, and by the technique of variable separation, $g_1(R)$, $g_2(\theta)$ and $g_3(\phi)$ can be shown to satisfy the following equations.

$$R^2 \frac{d^2 g_1}{dR^2} + 2R \frac{dg_1}{dR} + \left[-\gamma^2 R^2 - n(n+1) \right] g_1 = 0 \quad (A3)$$

$$\frac{1}{\sin\theta} \frac{d}{d\theta} \left(\sin\theta \frac{dg_2}{d\theta} \right) + \left[n(n+1) - \frac{m^2}{\sin^2\theta} \right] g_2 = 0 \quad (A4)$$

$$\frac{d^2 g_3}{d\phi^2} + m^2 g_3 = 0 \quad (A5)$$

The solution for $g_1(R)$ is given by

$$g_1(R) = \sqrt{\frac{\pi}{2\gamma R}} \begin{Bmatrix} I_{n+\frac{1}{2}}(\gamma R) \\ K_{n+\frac{1}{2}}(\gamma R) \end{Bmatrix} = \begin{Bmatrix} i_n(\gamma R) \\ k_n(\gamma R) \end{Bmatrix} \quad (A6)$$

where $I_{n+\frac{1}{2}}(\gamma R)$ is the first kind of modified Bessel function of order $n+\frac{1}{2}$, $K_{n+\frac{1}{2}}(\gamma R)$ is the second kind of modified Bessel function of order $n+\frac{1}{2}$. $i_n(\gamma R)$ and $k_n(\gamma R)$ can be considered as the first and second kind of modified spherical Bessel functions of order n .

The solution for $g_2(\theta)$ is

$$g_2(\theta) = P_n^m(\cos\theta) \quad (A7)$$

where $P_n^m(\cos\theta)$ is the associated Legendre's function of order n and degree m .

The solution for $g_3(\theta)$ is

$$g_3(\theta) = \begin{cases} \cos m\phi \\ \sin m\phi \end{cases} \quad (A8)$$

Therefore, the general solution for $g(R, \theta, \phi)$ is

$$g(R, \theta, \phi) = \sum_n \sum_m \begin{cases} i_n(\gamma R) \\ k_n(\gamma R) \end{cases} P_n^m(\cos\theta) \begin{cases} \cos m\phi \\ \sin m\phi \end{cases} \quad (A9)$$

It is possible to construct from $g(R, \theta, \phi)$ two possible solutions for \vec{E} which satisfy eq. (A1) and Maxwell's equations as follows. The first solution for \vec{E} is

$$\vec{M}(R, \theta, \phi) = \nabla \times (\vec{R}g) \quad (A10)$$

and the second solution for \vec{E} is

$$\vec{N}(R, \theta, \phi) = \frac{1}{\gamma} \nabla \times \vec{M}(R, \theta, \phi) \quad (A11)$$

These two solutions can be shown to satisfy eq. (A1) by direct substitution.

The substitution of eq. (A9) in eq. (A10) gives

$$\begin{aligned} \vec{M}_{\text{eomn}} &= \pm \frac{m}{\sin\theta} \begin{cases} i_n(\gamma R) \\ k_n(\gamma R) \end{cases} P_n^m(\cos\theta) \begin{cases} \sin m\phi \\ \cos m\phi \end{cases} \hat{\theta} \\ &\quad - \begin{cases} i_n(\gamma R) \\ k_n(\gamma R) \end{cases} \frac{P_n^m(\cos\theta)}{\partial\theta} \begin{cases} \cos m\phi \\ \sin m\phi \end{cases} \hat{\phi} \end{aligned} \quad (A12)$$

The substitution of eq. (A12) in eq. (A11) leads to

$$\begin{aligned}
 \vec{N}_{\delta^{mn}} &= \frac{n(n+1)}{\gamma R} \begin{Bmatrix} i_n(\gamma R) \\ k_n(\gamma R) \end{Bmatrix} P_n^m(\cos\theta) \begin{Bmatrix} \cos m\phi \\ \sin m\phi \end{Bmatrix} \hat{R} \\
 &+ \frac{1}{\gamma R} \frac{\partial}{\partial R} \begin{Bmatrix} R i_n(\gamma R) \\ R k_n(\gamma R) \end{Bmatrix} \frac{P_n^m(\cos\theta)}{\partial \theta} \begin{Bmatrix} \cos m\phi \\ \sin m\phi \end{Bmatrix} \hat{\theta} \\
 &+ \frac{m}{\gamma R \sin\theta} \frac{\partial}{\partial R} \begin{Bmatrix} R i_n(\gamma R) \\ R k_n(\gamma R) \end{Bmatrix} P_n^m(\cos\theta) \begin{Bmatrix} \sin m\phi \\ \cos m\phi \end{Bmatrix} \hat{\phi} \quad (A13)
 \end{aligned}$$

The subscript e and o stand for the even and odd \vec{M} and \vec{N} functions. The general solution for \vec{E} is any combination of even and odd \vec{M} and \vec{N} functions of any m and n .

It is noted that these solutions deviate from the conventional Mie series [8] in that the present solutions use modified spherical Bessel functions while Mie series uses ordinary spherical Bessel functions.

References

- [1] D. L. Moffatt and R. K. Mains, "Detection and discrimination of radar targets," IEEE Trans. on Ant. and Prop., Vol. AP-23, No. 3, pp. 358-367, May 1975.
- [2] A. J. Berni, "Target identification by natural resonance estimation," IEEE Trans. on Aerospace and Electronic Systems, Vol. AES-11, No. 2, pp. 147-154, March 1975.
- [3] J. D. Young, "Radar imaging from ramp response signatures," IEEE Trans. on Ant. and Prop., Vol. AP-24, No. 3, pp. 276-282, May 1976.
- [4] K. A. Shubert, J. D. Young and D. L. Moffatt, "Synthetic radar imagery," IEEE Trans. on Ant. and Prop., Vol. AP-25, No. 4, pp. 477-483, July 1977.
- [5] C. W. Chuang and D. L. Moffatt, "Natural resonance of radar target via Prony's method and target discrimination," IEEE Trans. on Aerospace and Electronic Systems, Vol. AES-12, No. 5, pp. 583-589.
- [6] M. L. Van Blaricum and R. Mittra, "A technique for extracting the poles and residues of a system directly from its transient response," IEEE Trans. on Ant. and Prop., Vol. AP-23, No. 6, pp. 777-781, November 1975.
- [7] K. M. Chen, D. P. Nyquist, D. Westmoreland, Che-I Chuang, and B. Drachman, "Radar waveform synthesis for target discrimination," presented at 1981 International IEEE/AP-S Symposium, Los Angeles, CA, June 16-19, 1981.
- [8] J. A. Stratton, Electromagnetic Theory, McGraw-Hill, 1941.
- [9] Abramowitz and Stegun, ed., Handbook of Mathematical Functions, AMS 55, National Bureau of Standards, 1964.
- [10] G. N. Watson, "The diffraction of electric waves by the earth," Proc. Roy. Soc. London, (A) 95, 83, 1918.
- [11] E. M. Kennaugh, "The scattering of short EM pulse by a conducting sphere," the Proc. of IRE, 49, 380, January 1961.

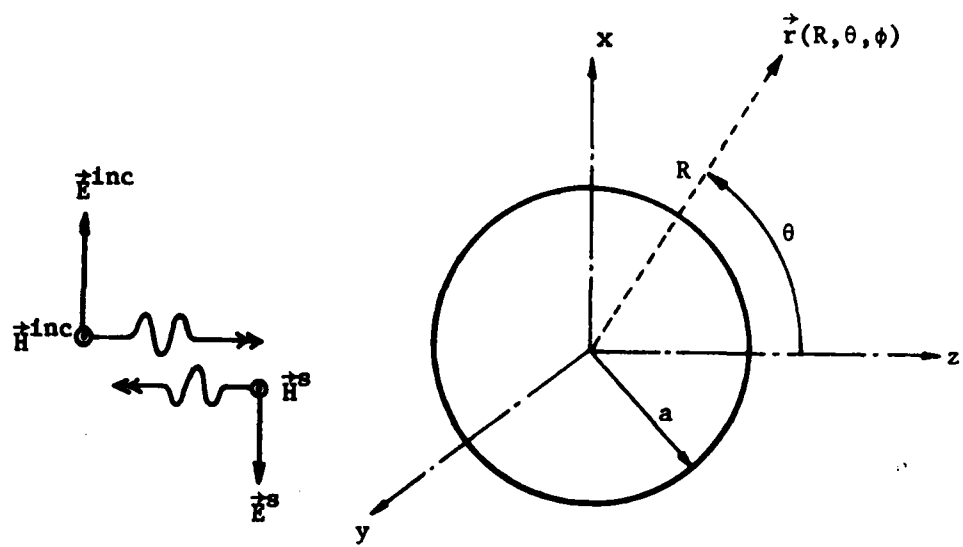


fig. 1 A perfectly conducting sphere of radius a is illuminated by a radar signal propagating in the $+z$ -direction.

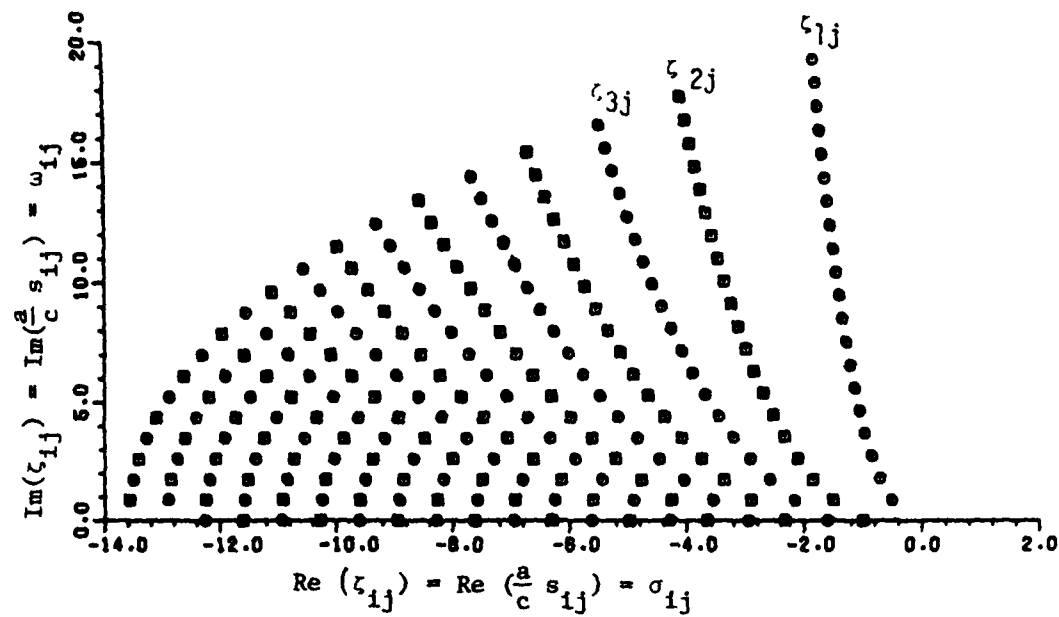


fig. 2 Natural frequencies of a conducting sphere; the poles are grouped into branches in the S-plane

Table 1: Poles of the first and second branches shown in the above figure and the corresponding residues.

j	poles of 1st branch $\zeta_{1j} = \sigma_{1j} + j\omega_{1j}$		residues at ζ_{1j}		poles of 2nd branch $\zeta_{2j} = \sigma_{2j} + j\omega_{2j}$		residues at ζ_{2j}	
	σ_{1j}	ω_{1j}	a_{1j}^r	a_{1j}^i	σ_{2j}	ω_{2j}	a_{2j}^r	a_{2j}^i
0	-	-	-	-	-1.000	0.	3.000	0.
1	-.5000	.8660	0.	1.732	-1.500	.8660	0.	8.660
2	-.7020	1.807	-2.757	.5773	-1.839	1.754	-18.05	2.364
3	-.8430	2.758	-1.879	-3.557	-2.104	2.657	-10.29	-31.07
4	-.9540	3.715	3.734	-3.825	-2.325	3.571	45.70	-27.74
5	-1.048	4.676	6.145	2.920	-2.516	4.493	58.40	57.23
6	-1.129	5.642	-.8226	8.327	-2.686	5.421	-57.95	104.2
7	-1.201	6.610	-9.734	2.529	-2.839	6.354	-163.4	-37.51
8	-1.267	7.580	-6.852	-9.726	-2.979	7.292	-15.41	-228.3
9	-1.327	8.553	7.700	-11.51	-3.109	8.233	284.3	-110.1
10	-1.382	9.527	15.53	3.468	-3.230	9.177	250.3	309.9
11	-1.434	10.50	2.777	17.93	-3.343	10.12	-278.2	429.4
12	-1.483	11.48	-17.67	10.41	-3.450	11.07	-627.6	-161.8
13	-1.528	12.46	-18.13	-14.09	-3.551	12.03	-60.65	-807.6
14	-1.572	13.44	7.004	-24.65	-3.647	12.98	919.4	-396.4
15	-1.613	14.42	28.20	-3.078	-3.739	13.94	828.8	902.5
16	-1.653	15.40	14.88	27.57	-3.827	14.89	-697.2	1313.
17	-1.691	16.38	-21.84	26.61	-3.912	15.85	-1771.	-259.0
18	-1.727	17.36	-35.97	-11.00	-3.993	16.81	-425.9	-2096.
19	-1.762	18.34	-3.843	-40.83	-4.071	17.77	2165.	-1325.

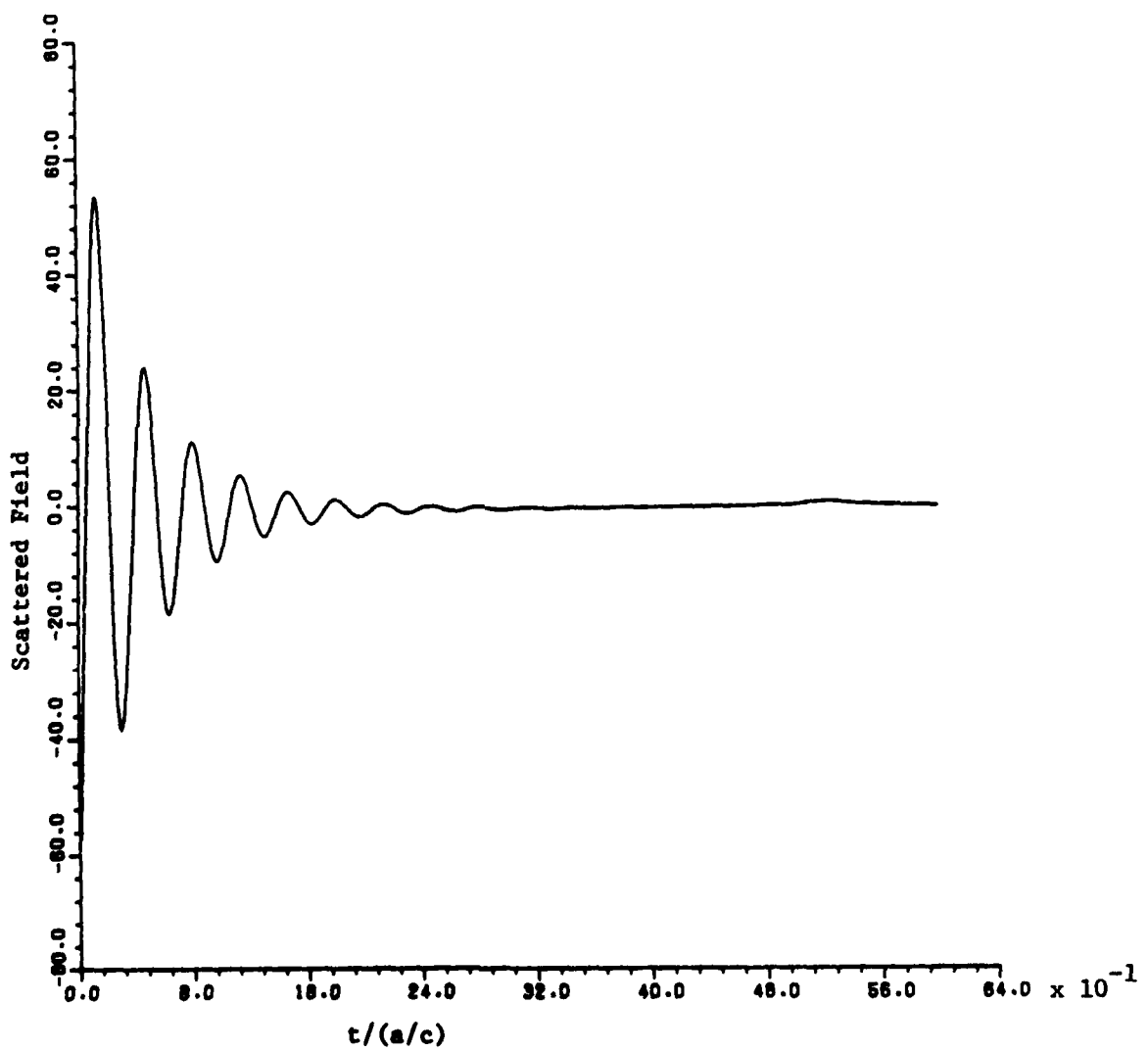


fig. 3 The impulse response of a conducting sphere of radius a computed from the first 19 pairs of poles of the first branch.

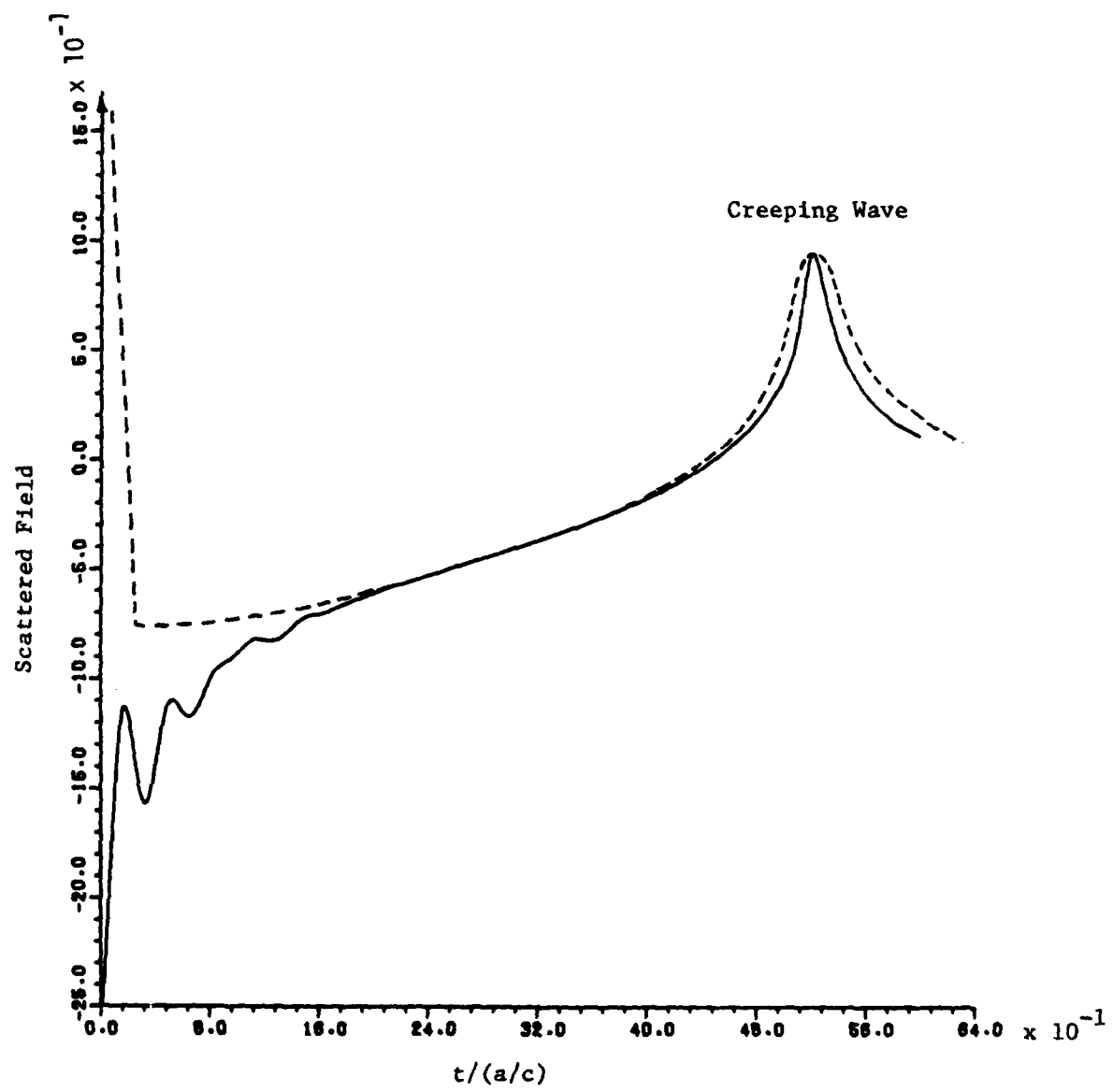


fig. 4 The impulse response of a conducting sphere of radius a computed from the first 19 poles of the first branch and the correction term of eq. (29). The impulse response shown by the dotted line is obtained with the Fourier-numerical method.

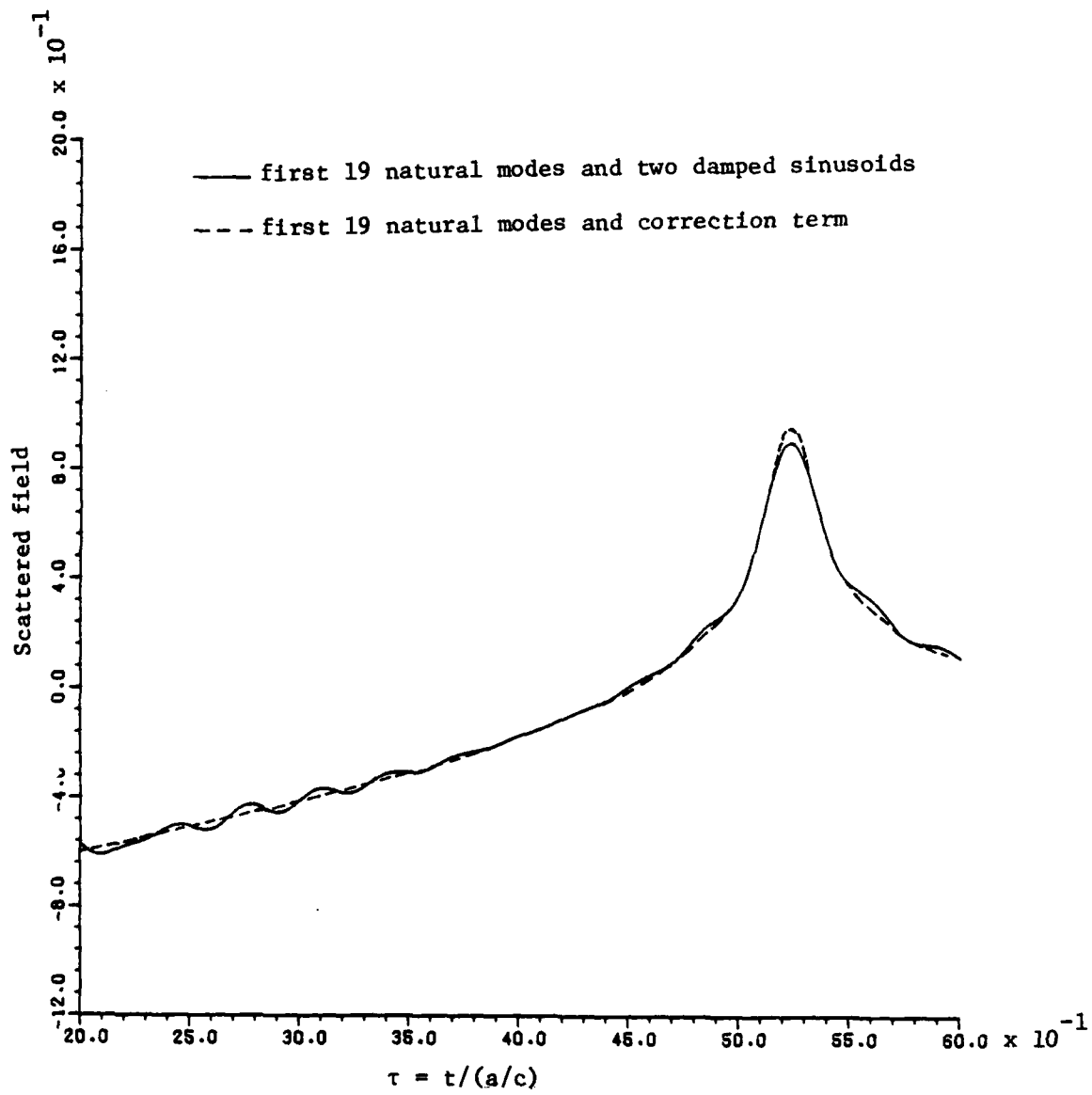


fig. 5 Approximate impulse response for $\tau > 2$ constructed with the first 19 natural modes of the first branch poles and two damped sinusoids which approximate the correction term.

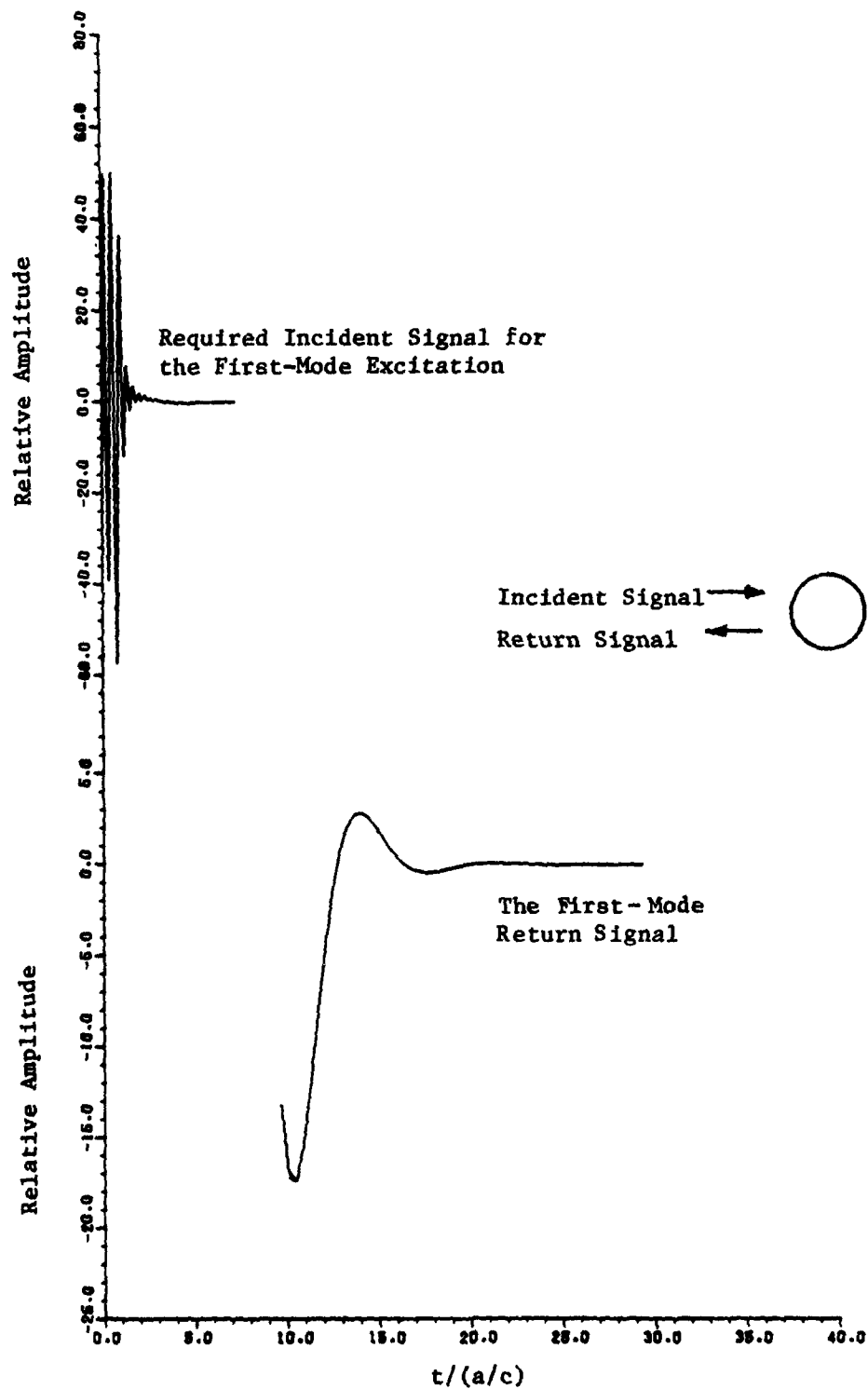


fig. 6 The required incident signal for exciting the first natural mode of a sphere, and the return signal which contains only the first natural mode.

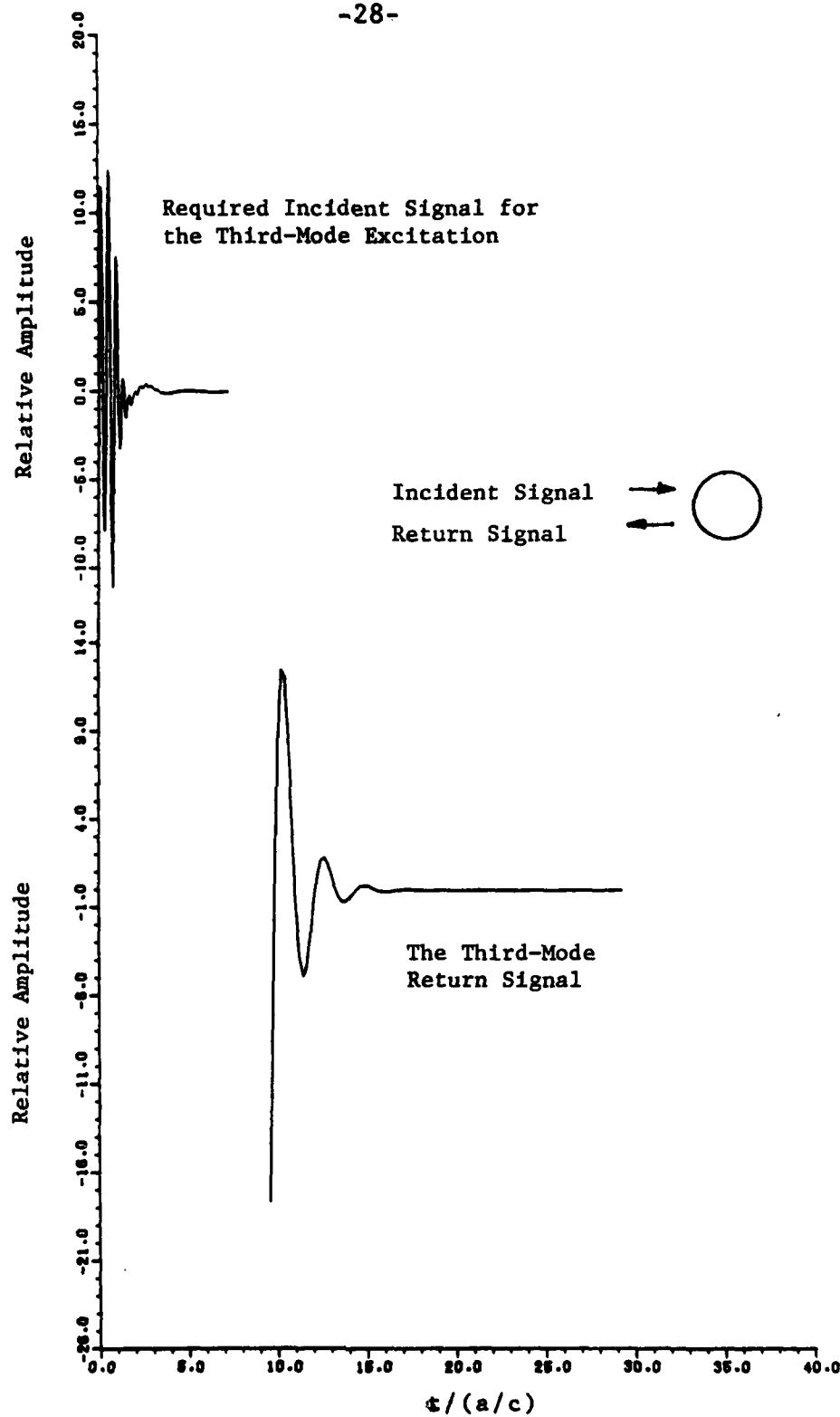


fig. 7 The required incident signal for exciting the third natural mode of a sphere, and the return signal which contains only the third natural mode.

Table 2. Natural Modes Used to Construct the Required Incident Signals for Exciting the First and the Third Mode Backscatters.

$$E^i(\tau) = \sum_{n=1}^{21} a_n e^{-\omega_n \tau} \cos(\omega_n \tau + \phi_n), \quad 0 < \tau < 7.26.$$

$E^i(\tau)$ for First-Mode Excitation		E^i for Third-Mode Excitation	
n	Natural Mode Components	n	Natural Mode Components
1	$0.2703 e^{-0.5\tau} \cos(0.866\tau - 91.86^\circ)$	1	$0.2624 e^{-0.5\tau} \cos(0.866\tau + 171.1^\circ)$
2	$0.1085 e^{-0.702\tau} \cos(1.807\tau + 128.11^\circ)$	2	$0.2972 e^{-0.702\tau} \cos(1.807\tau + 138.72^\circ)$
3	$0.1245 e^{-0.843\tau} \cos(2.758\tau + 90.38^\circ)$	3	$2.743 e^{-0.843\tau} \cos(2.758\tau - 83.66^\circ)$
4	$0.1394 e^{-0.954\tau} \cos(3.715\tau + 46.48^\circ)$	4	$0.3245 e^{-0.954\tau} \cos(3.715\tau + 68.75^\circ)$
5	$0.1639 e^{-1.048\tau} \cos(4.676\tau - 5.45^\circ)$	5	$0.2945 e^{-1.048\tau} \cos(4.676\tau + 21.09^\circ)$
6	$0.2184 e^{-1.129\tau} \cos(5.642\tau - 62.5^\circ)$	6	$0.2880 e^{-1.129\tau} \cos(5.642\tau - 48.45^\circ)$
7	$0.3265 e^{-1.201\tau} \cos(6.61\tau - 114.95^\circ)$	7	$0.4556 e^{-1.201\tau} \cos(6.61\tau - 120.05^\circ)$
8	$0.4909 e^{-1.267\tau} \cos(7.58\tau - 161.2^\circ)$	8	$0.8078 e^{-1.267\tau} \cos(7.58\tau - 172.15^\circ)$
9	$0.6914 e^{-1.327\tau} \cos(8.55\tau + 155.26^\circ)$	9	$1.264 e^{-1.327\tau} \cos(8.55\tau + 143.81^\circ)$
10	$0.9013 e^{-1.382\tau} \cos(9.527\tau + 112.82^\circ)$	10	$1.752 e^{-1.382\tau} \cos(9.527\tau + 102.09^\circ)$
11	$1.108 e^{-1.434\tau} \cos(10.5\tau + 69.4^\circ)$	11	$2.233 e^{-1.434\tau} \cos(10.5\tau + 59.56^\circ)$
12	$1.304 e^{-1.483\tau} \cos(11.48\tau + 22.87^\circ)$	12	$2.687 e^{-1.483\tau} \cos(11.48\tau + 13.75^\circ)$
13	$1.507 e^{-1.528\tau} \cos(12.46\tau - 26.37^\circ)$	13	$3.151 e^{-1.528\tau} \cos(12.46\tau - 35.07^\circ)$
14	$1.839 e^{-1.572\tau} \cos(13.44\tau - 78.36^\circ)$	14	$3.895 e^{-1.572\tau} \cos(13.44\tau - 86.90^\circ)$
15	$2.337 e^{-1.613\tau} \cos(14.42\tau - 128.73^\circ)$	15	$5.025 e^{-1.613\tau} \cos(14.42\tau - 137.11^\circ)$
16	$3.010 e^{-1.653\tau} \cos(15.40\tau - 173.66^\circ)$	16	$6.560 e^{-1.653\tau} \cos(15.40\tau + 178.25^\circ)$
17	$3.634 e^{-1.691\tau} \cos(16.38\tau + 148.54^\circ)$	17	$8.011 e^{-1.691\tau} \cos(16.38\tau + 140.79^\circ)$
18	$3.794 e^{-1.727\tau} \cos(17.36\tau + 125.69^\circ)$	18	$8.443 e^{-1.727\tau} \cos(17.36\tau + 118.21^\circ)$
19	$4.933 e^{-1.762\tau} \cos(18.34\tau + 156.14^\circ)$	19	$11.00 e^{-1.762\tau} \cos(18.34\tau + 148.72^\circ)$
20	$9.203 e^{-2.0\tau} \cos(18.891\tau - 58.56^\circ)$	20	$20.45 e^{-2.0\tau} \cos(18.891\tau - 65.54^\circ)$
21	$0.193 e^{-0.55\tau} \cos(19.50\tau - 79.67^\circ)$	21	$0.0437 e^{-0.55\tau} \cos(19.50\tau - 86.75^\circ)$

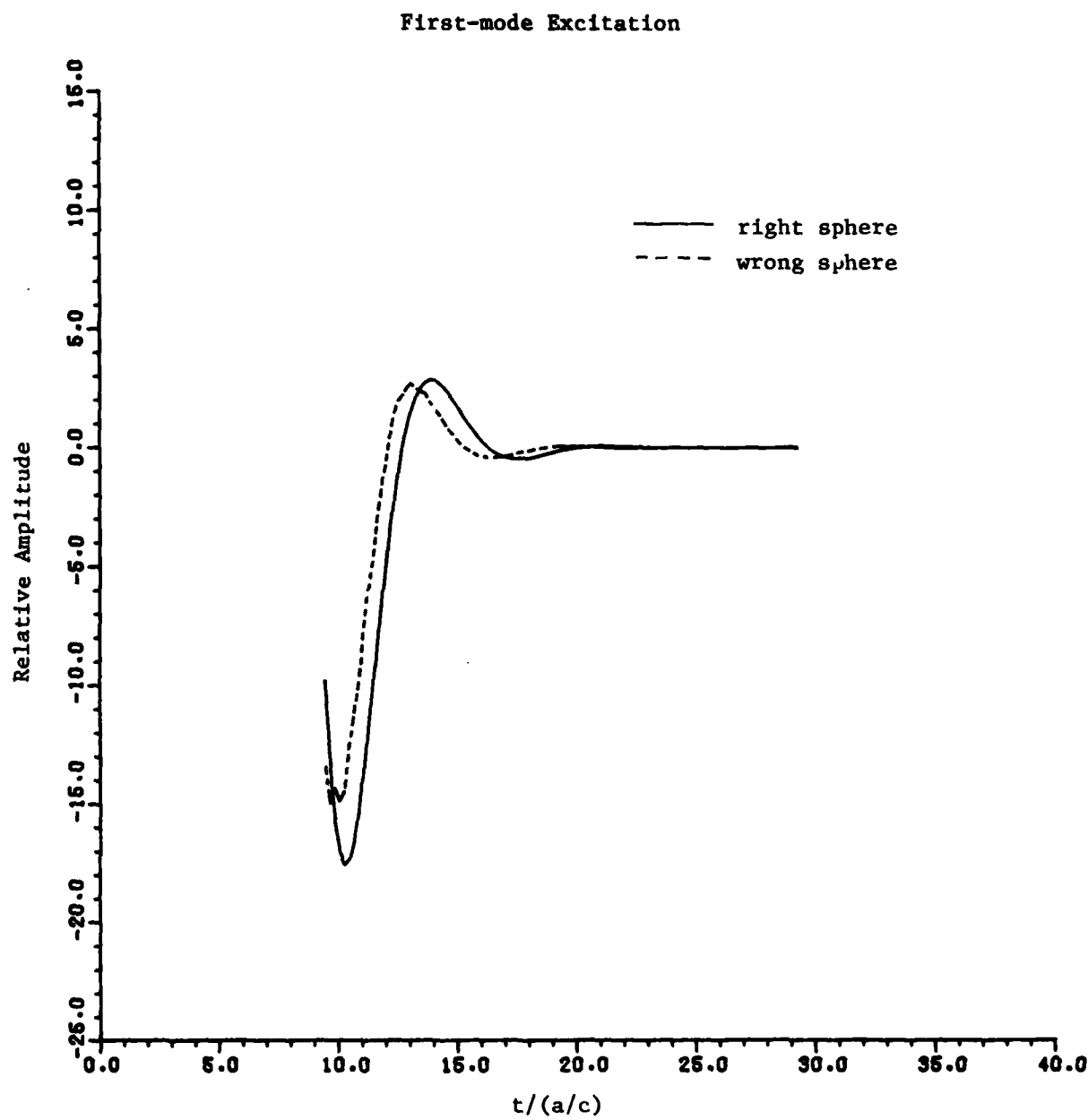


fig. 8 The return signals from the right sphere and a wrong sphere which radius is 10% smaller than that of the right sphere when they are illuminated by the incident signal synthesized to excite the first natural mode of the right sphere.

Third-mode Excitation

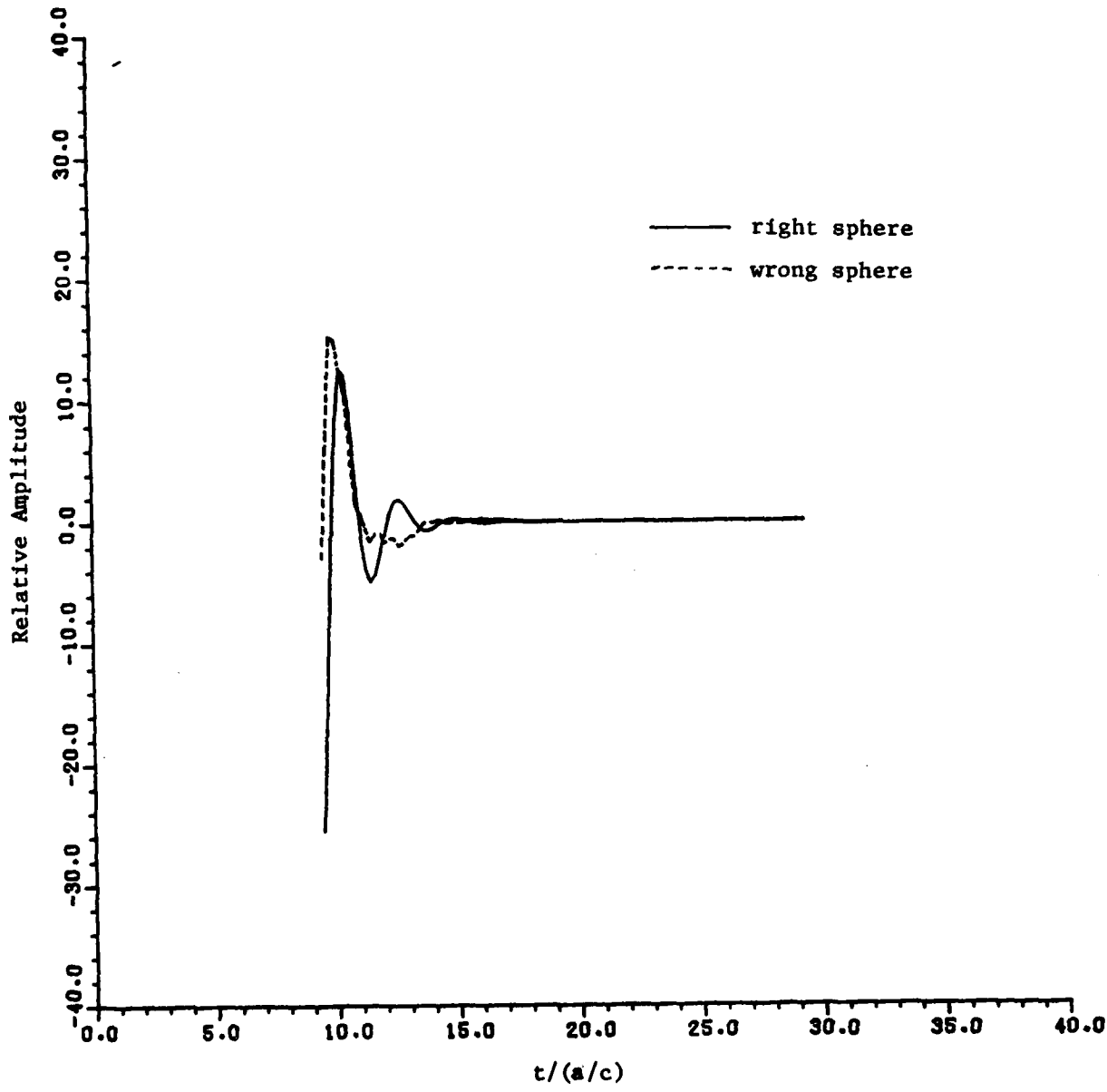


fig. 9 The return signals from the right sphere and a wrong sphere which radius is 10% smaller than that of the right sphere when they are illuminated by the incident signal synthesized to excite the third natural mode of the right sphere.

PART 3

WORK IN PROGRESS, FUTURE PLANS AND
PUBLICATION LIST

1. Work in Progress

The study on the radar waveform synthesis for exciting a single-mode backscatter from a normally oriented, infinite cylinder is in its final stage. The results obtained up to date are briefly outlined below.

A radar signal propagating in the $+x$ -direction is incident on an perfectly conducting, infinite cylinder of radius a with its axis located along the z axis. The electric field of the incident radar signal, in its Laplace transform, is assumed to be

$$\vec{E}^i(\vec{r}, s) = \hat{y} F(s) e^{-\gamma a} e^{-\gamma r \cos \phi} \quad (1)$$

where $F(s)$ is an unknown waveform function to be synthesized in such a way that $\vec{E}^i(\vec{r}, s)$ excites a single-mode backscatter from the cylinder, and $\gamma = s/c$.

The backscattered electric field can be obtained, through a long theoretical development, to be

$$\vec{E}^s(\vec{r}, s) = -\hat{y} F(s) \sqrt{\frac{\pi a}{2r_\infty}} e^{-\gamma(r_\infty - a)} H(s) \quad (2)$$

where r_∞ is the distance between the observation point and the cylinder and $H(s)$ is the transfer function. $H(s)$ can be expressed as

$$H(s) = \sum_{n=0}^{\infty} \epsilon_n \frac{I'_n(\xi) e^{-2\xi}}{K'_n(\xi) \sqrt{\xi}} \quad (3)$$

where $I'_n(\xi)$ and $K'_n(\xi)$ are the derivatives of the first and the second kind of the modified Bessel functions, $\epsilon_0 = 1$ for $n=0$ and $\epsilon_n = 2$ for $n > 0$, and $\xi = \gamma a = s(a/c)$.

The impulse response of the cylinder is obtained by inverting $H(s)$. To invert $H(s)$, the first step is to find the poles of $H(s)$ or the roots of $K'_n(\xi)$. The roots of $K'_n(\xi)$ are shown in Fig. 1. The next step is to perform the integration around the branch cut of $H(s)$ along the negative real axis on the s -plane. By so doing, the impulse response of the cylinder $h(t)$ can be expressed as

$$h(t) = \sum_{n=0}^{\infty} \sum_{i=1}^{n \text{ or } n+1} 2 \operatorname{Re}(a_{ni} e^{\xi_{ni} t}) + \sum_{n=0}^{\infty} \frac{1}{\pi} \int_0^{\infty} \frac{e^{-\xi(t-2)} I_n'(\xi) K_n'(\xi)}{\sqrt{\xi[K_n(\xi) + \pi^2 I_n(\xi)]}} d\xi \quad (4)$$

where ξ_{ni} is the i th root of the $K_n'(\xi)$ function and a_{ni} is the residue of $H(s)$ at ξ_{ni} . The first term of eq. (4) is the sum of all the natural modes and the second is a line integral which comes from the integration around the branch cut.

Numerically, we have found that the sum of a finite number of natural modes plus the numerical integration of the line integral of eq. (4) given an approximate impulse response which is quite accurate for the late-time period. Preliminary results of the approximate impulse response of the cylinder is shown in Fig. 2.

We are in the process of calculating the required incident signals for exciting various single-mode backscatters. Once these required incident signals are obtained, the return signals can be obtained by convoluting the incident signals with the impulse response of the cylinder. We expect to complete these calculations in the near future.

2. Future Plans

The following topics will receive major attention in the future.

1. We will initiate the study on the radar waveform synthesis for exciting single-mode backscatters from two coupled wire targets which are oriented at an angle and illuminated by an incident radar signal at an arbitrary direction. The case of special interest will be a wire target placed over a ground plane and illuminated by an incident signal. Results of this study will guide the experiment to be conducted on a ground plane.

2. We will initiate the study on the cross-wire structure which simulates an aircraft.
3. We will design an experimental setup for conducting the experiment.

3. Personnel

The following personnel have participated in this research program.

- (1) Kun-Mu Chen, Professor and principal investigator.
- (2) Dennis P. Nyquist, Professor and senior investigator.
- (3) Byron Drachman, Associate Professor of mathematics, consultant.
- (4) Che-I Chuang, Graduate Assistant.
- (5) Doug V. Westmoreland, Graduate Assistant.

4. Publication

Results of this research program have been published in the following papers.

- (1) K.M. Chen, "Radar Waveform Synthesis Method -- A New Radar Detection Scheme", presented at 1980 IEEE International AP-S Symposium, Laval University, Quebec City, Canada, June 2-6, 1980.
- (2) K.M. Chen, D.P. Nyquist, C-I Chuang, D. Westmoreland, and B. Drachman, "Incident-Waveform Synthesis for Single-Mode Scattering by an Obliquely Illuminated, Thin-Wire Cylinder", Presented at 1981 National Radio Science Meeting, Boulder, Colorado, Jan. 12-16, 1981.
- (3) K.M. Chen and D. Westmoreland, "Impulse Response of a Conducting Sphere Based on Singularity Expansion Method", Proceedings of IEEE, Vol. 69, No. 6, pp. 747-750, June 1981.
- (4) K.M. Chen, "Radar Waveform Synthesis Method - A New Radar Detection Scheme", to appear in IEEE Trans. on Antennas and Propagation, July 1981.
- (5) K.M. Chen, D.P. Nyquist, D. Westmoreland, Che-I Chuang, and B. Drachman, "Radar Waveform Synthesis for Target Discrimination", presented at 1981 IEEE International AP-S Symposium, Los Angeles, California, June 16-19, 1981.

- (6) K.M. Chen and D. Westmoreland, "Synthesis of Radar Signal for Exciting a Single-Mode Backscatter from a Sphere", presented at 1981 National Radio Science Meeting, Los Angles, California, June 16-19, 1981.
- (7) K.M. Chen, D.P. Nyquist, D. Westmoreland, Che-I Chuang, and B. Drachman, "Radar Waveform Synthesis for Single-Mode Scattering by a Thin Cylinder and Application for Target Discrimination", submitted to IEEE Trans. on Antennas and Propagation.

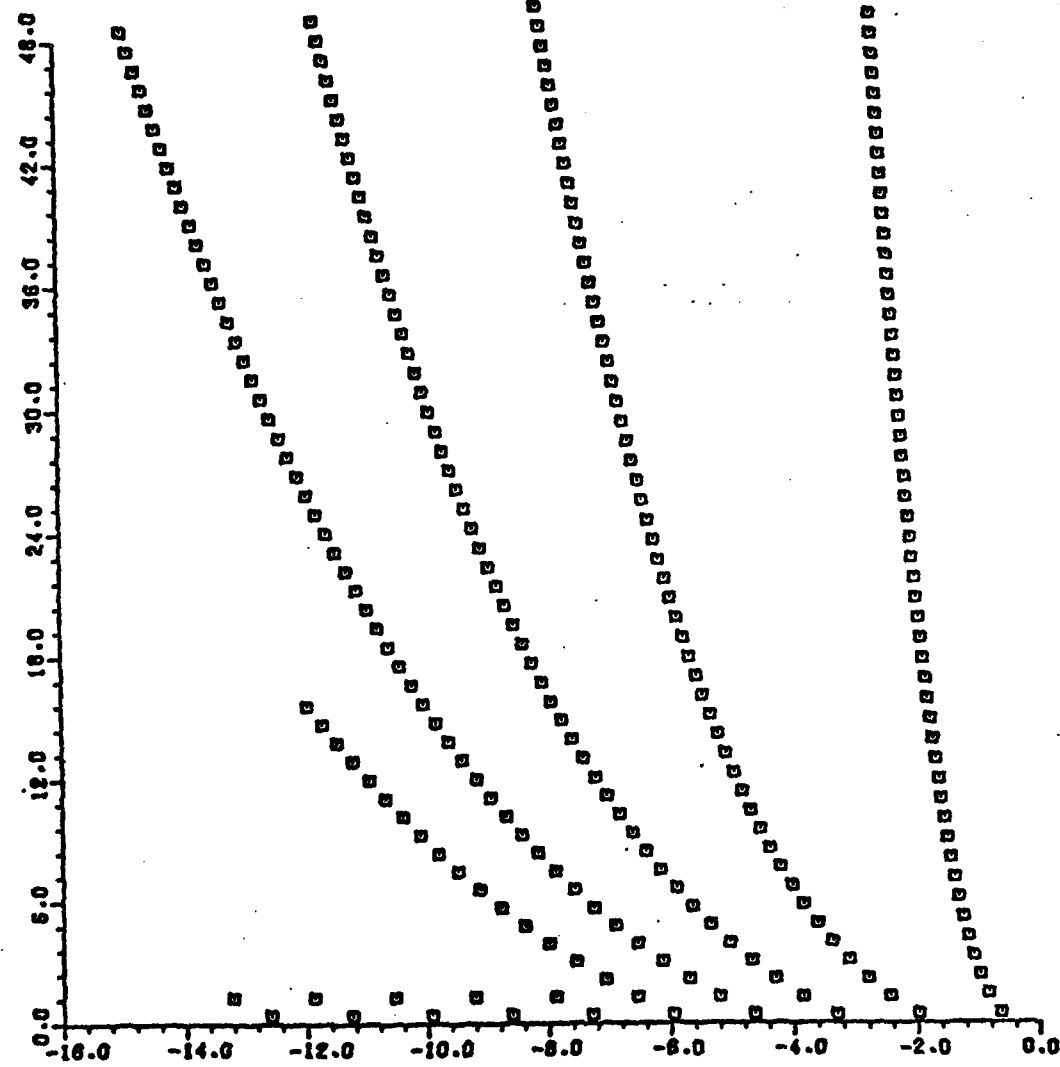


fig. 1. The Roots of $K_n'(z) = 0$ in the Second Quadrant

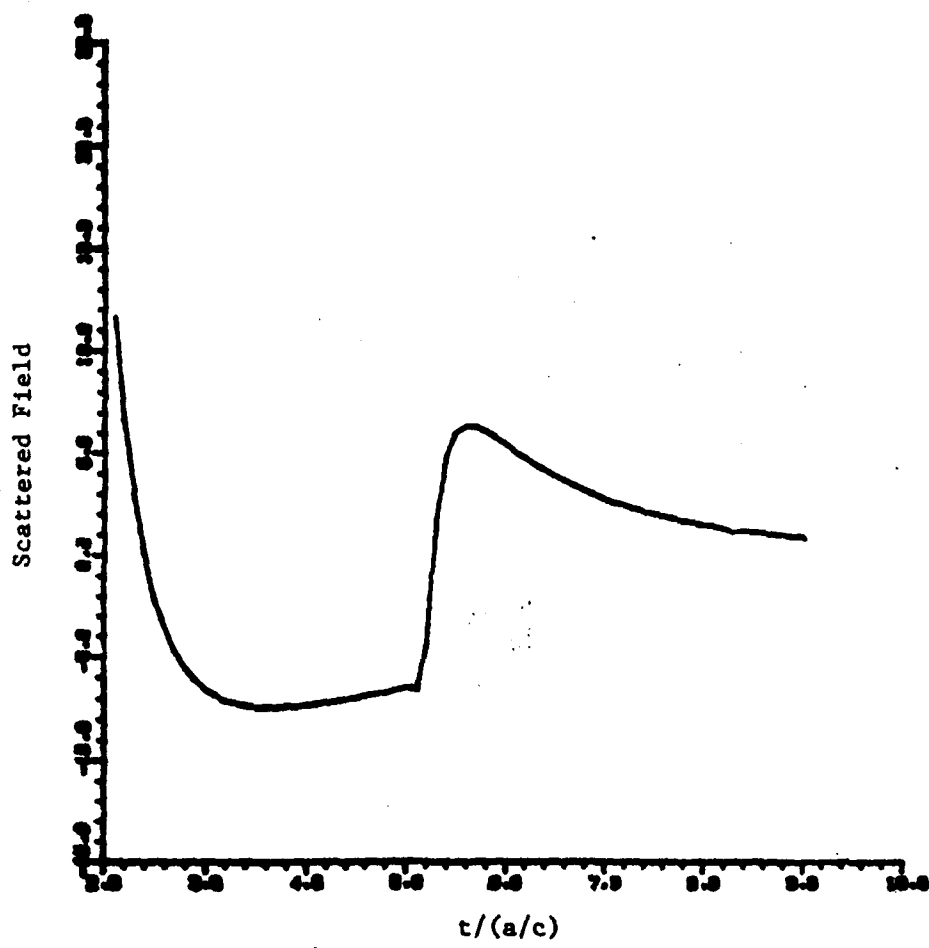


fig. 2. The impulse response of an infinite cylinder of radius a when the impulse signal is incident normally on the cylinder.